Current Research (2024) Newfoundland and Labrador Department of Industry, Energy and Technology Geological Survey, Report 24-1, pages 1-30

VOLCANIC-FACIES MAPPING AND RELATED HYDROTHERMAL ALTERATION STUDIES OF THE BUCHANS CAMP, SOUTHERN BUCHANS–ROBERTS ARM BELT, CENTRAL NEWFOUNDLAND

R.L. Allen, M. Schofield[1] and G.W. Sparkes[1]
Volcanic Resources AB, Enköping, Sweden
[1]Mineral Deposits Section

ABSTRACT

The application of volcanic-facies mapping utilizing detailed graphic logging of diamond-drill core represents a new approach to subdividing the Buchans stratigraphy, and when combined with whole-rock geochemistry, provides an effective means of outlining several ore horizons developed within the immediate Buchans area. This new approach highlights four submarine rhyolite dome–cryptodome eruption packages or volcanoes, defined as four stratigraphic members of the VMS host succession. These eruption packages are distinguished based on a combination of their physical characteristics and immobile-element ratios obtained from lithogeochemical analyses. One eruption package occurs at the top of the Ski Hill Formation (Intermediate Footwall member). The overlying Buchans River Formation is subdivided into a lower Buchans River Formation comprising two rhyolite dome–cryptodome packages, one in the eastern part of the area (Oriental-Sandfill member) and the other in the west (Clementine member), and an upper Buchans River Formation dominated by one rhyolite dome–cryptodome package that covers the entire area (Buchans Camp member). The massive sulphide ores and ore-clast breccia units at Buchans formed in response to hydrothermal, volcanic and tectonic events during the emplacement of these rhyolite dome–cryptodome volcanoes. Two camp-wide and three additional local ore horizons are distinguished. These ore horizons occur on top of the first, second and third rhyolite dome–cryptodome eruption packages and within the third and the basal 10s of metres of the fourth rhyolite dome–cryptodome eruption package. A notable transition in the felsic volcanic rocks within the overall stratigraphic sequence, from transitional through intermediate transitional-calc-alkaline to calc-alkaline, demonstrates an evolution to more evolved felsic magmatic compositions within increasingly younger stratigraphic units.

*Short wavelength infrared (SWIR) studies of the "sericitic" alteration commonly noted in association with the development of massive sulphide illustrates the formation of shorter wavelength white mica minerals (*e.g.*, muscovite, muscovitic-illite) proximal to mineralization. The collection of systematic downhole measurements highlight the decreasing Al-OH wavelength feature with decreasing distance from mineralization, which can be illustrated numerically by plotting the Al-OH scalar variable against downhole depth. Sharp shifts in this spectral feature locally highlight the structural juxtaposition of contrasting alteration assemblages, and aids in the recognition of significant fault structures.*

INTRODUCTION

Recent studies of the local stratigraphy within the Buchans camp has applied volcanic-facies mapping to define the characteristics of individual rock units developed in the area (*cf.* Allen and Schofield, 2023). This report represents a summary of this work, combined with short wavelength infrared (SWIR) spectrometry studies focused on the hydrothermal alteration associated with the formation of the volcanogenic massive sulphide (VMS) deposits. In total, eight groups of facies were identified (*see* below); these include diffusely stratified rhyolitic lithic breccias and quench-brecciated submarine lava, interpreted as submarine hydrothermal eruption breccias and hyaloclastite, respectively. The latter had previously been mapped as "crystal tuffs" (*e.g.*, Jambor, 1987), and has proven to be more common at Buchans than pyroclastic facies (*i.e.*, crystal tuffs).

VOLCANIC-FACIES MAPPING

Volcanic facies have not previously been defined at Buchans, instead previous workers named volcanic rocks based on composition and inferred genesis; most rocks were named tuffs or tuff-breccias, implying (although perhaps not always intentionally) a pyroclastic origin. In the current study, volcanic facies were defined by synthesis of the char-

acteristics of the rock units defined on new volcanological "graphic-style" drillcore logs for 34 drillholes from the Buchans area.

Each facies is defined in terms of interpreted volcanic composition, mineralogical composition (phenocryst type and amount), grain size and/or phenocryst size, sorting, components (pumice, lithic clasts, crystals), textures (spherulitic, evidence of glassy character, porphyritic), bedforms and structures, contact relationships, geometry, and range in the type, style and intensity of alteration. Each of these characteristics, and how they have been described, are summarized in Table 1. A summary of the main facies and an interpretation of their origin is in Table 2. For this study, the term "vitric" is used to refer to all originally glassy materials: pumice and glass shards in pyroclastic rocks and some lavas, and dense glass and glassy blocks in lavas and shallow intrusions. The term "polychromatic" is used to describe clastic rocks that show variable colour due to variation in the intensity and mineralogy of alteration from clast to clast and even within individual clasts, imparting a superficially polymict appearance to the rock (Gary McArthur *pers. comm.*, 1980).

REGIONAL GEOLOGY

The geology of the southern Buchans–Roberts Arm Belt (BRAB), primarily confined to the area north of Beothuk Lake (formerly known as Red Indian Lake), has most recently been discussed by Zagorevski and Rogers (2008, 2009), Zagorevski *et al.* (2007, 2015, 2016) and Sparkes *et al.* (2021). From this work, the geology of the area has been subdivided into five units, consisting of: the Lloyds/Harry's River Ophiolite and Hungry Mountain complexes, and the Mary March Brook, Buchans and the Red Indian Lake groups (Figure 1). The Mary March Brook group (formerly the Seal Pond formation of Zagorevski *et al.* (2007) and the Little Sandy Sequence of Thurlow and Swanson (1981)) includes rocks of the Lundberg Hill Formation of Thurlow and Swanson (1987). Thurlow and Swanson (1987) subdivided the Buchans Group into the Lundberg Hill, Ski Hill, Buchans River and Sandy Lake formations. Only rocks located within the immediate Buchans area are discussed in detail, as they are relevant to the current study (Figure 2). This report utilizes the stratigraphic terminology of Thurlow and Swanson (1987) for the rocks in the Buchans area, allowing for easier comparison with historical reports.

The Buchans Group is composed of calc-alkalic basaltic and rhyolitic rocks of continental-arc affinity, along with characteristic granitoid-bearing conglomerate and debris flows (Thurlow and Swanson, 1987; Swinden *et al.*, 1997; Zagorevski *et al.*, 2015, 2016). Sensitive high-resolution ion microprobe (SHRIMP) geochronological data from volcanic rocks within lower stratigraphic levels of the group range from 465 ± 4 to 463 ± 4 Ma, while a felsic crystal tuff from stratigraphically higher in the sequence is dated at 462 ± 4 Ma (Zagorevski *et al.*, 2015). Thermal ionization mass spectrometry (TIMS) dating of granitoid clasts from within the debris flows of the Buchans mine area provide an age of 464 ± 4 Ma (Whalen *et al.*, 2013). TIMS dating of a felsic volcanic rock located stratigraphically below one of the mineralized debris flows at the MacLean deposit provides

Table 1. Facies characteristics used for describing volcaniclastic rocks in the Buchans area

Facies characteristic	Sub-types and description
Interpreted composition	Rhyolite, dacite, andesite, basalt
Phenocrysts	Percentage and average size of each phenocryst mineral
Grain size	Breccia/conglomerate, sand, silt, mud
Clast composition	Monomict, polymict, pumice-rich/lithic-rich
Clast distribution/framework	Clast/matrix-supported
Sorting	Well, moderately, poorly
Clast organization	Jigsaw (*in situ* breccia), disorganized
Fracture pattern in jigsaw breccias	Random, sheeted, branching, network
Clast margins and fractures	Planar, curviplanar, serrated, hackly, undulating
Clast textures	Pumiceous, perlitic, spherulitic, felsitic, stoney
Clast shapes	Polygonal, blocky, lenticular, slabby, splinter
Matrix	Mud, silty, sandy, even grained, pumiceous, crystal- and/or lithic-rich
Bedforms and structures	Massive, planar/cross-stratified, normal graded
Geometry	Tabular, sheet, mound, lens, pod, dyke, pipe
Contacts with adjacent facies	Sharp, gradational, mixed, planar, irregular
Alteration and veining	Veins cut by clast margins, multiple generations

Table 2. Volcanic facies identified at Buchans and related interpretations

Volcanic facies	Subclass	Genetic classification/Interpretation
1 Coherent	a) Massive to flow banded, porphyritic to aphyric	Lava or shallow intrusion
	b) Massive, amygdales increase upward	Mafic lava flow
2 Massive monomict vitric breccia	a) Jigsaw-fit texture, altered glassy, diffuse curviplanar margins	*In situ* hyaloclastite
	b) Sediment matrix, local jigsaw texture, glassy, curviplanar margins	Intrusive hyaloclastite (peperite) or slumped hyaloclastite/peperite
	c) No jigsaw texture, matrix- to clast-supported, normal-graded well-sorted top, ragged elongate vitric (pumice) clasts	Subaqueous mass flow from magmatic/phreatomagmatic pyroclastic eruption
	d) No jigsaw texture, matrix supported, ragged elongate vitric (pumice) clasts, perlite/spherulites, eutaxitic matrix	Welded pyroclastic flow
3 Massive monomict lithic breccia	a) Jigsaw-fit texture, serrated-sinuous fractures, altered	*In situ* hydrothermal breccia
	b) Polychromatic, angular-subrounded, blocky-slabby-wedge clasts, serrated margins, moderately sorted, may contain massive sulphide clasts; no jigsaw texture	Hydrothermal or phreatic eruption breccia
	c) Slurry texture (very poor sorting), local sorting, sharp intrusive contacts, may contain sulphide clasts	Hydrothermal breccia dyke
	d) Flow-banded blocky clasts, clast-supported, grades to coherent lava	Flow breccia
	e) Mafic, >25 cm rounded domains, chilled margins, clast-supported	Pillow lava and/or pillow breccia
	f) Mafic, <25 cm fluidal lobes, chilled, matrix-supported	Fire fountain deposit
4 Stratified monomict vitric (± lithic) breccia	a) Altered glassy, curviplanar margins	Re-sedimented hyaloclastite
	b) Normal-graded beds, monomict juvenile component	Deep-water sedimented pyroclastic debris or re-sedimented hyaloclastite
	c) Traction stratification, moderate-well sorted	As above; on proximal apron or shallow water
5 Stratified monomict lithic breccia	a) Polychromatic, angular-subrounded, blocky-slabby-wedge clasts, serrated margins, moderate-well sorted, may contain massive sulphide clasts	Hydrothermal or phreatic eruption breccia; traction within breccia dyke
6 Massive to stratified polymict lithic breccia	a) Poorly sorted, clast- or matrix-supported	Mass flow of reworked debris
	b) Moderate-well sorted	Traction sedimentation, reworked debris
	c) Crystal-lithic rich, subordinate pumice	Reworked pyroclastic debris
	d) Polychromatic, angular-subrounded, blocky-slabby-wedge clasts, serrated margins, moderately sorted, ± massive sulphide clasts	Hydrothermal or phreatic eruption breccia
	e) Slurry texture (very poor sorting), local sorting and clast alignment/stratification, sharp intrusive contacts	Hydrothermal breccia dyke
7 Massive to stratified polymict lithic breccia-conglomerate	a) Moderately to poorly sorted, clast- to matrix-supported, some rounded clasts, ± massive sulphide clasts	Mass flow of reworked debris; rounded clasts: distal shallow source
8 Siltstone–sandstone	a) Vitric, diffuse stratified, local pumice layers	Suspension settled pyroclastic ash
	b) Lithic, not crystal enriched, massive to stratified, moderate to well sorted, gravelly sandstone	Sedimented hydrothermal/phreatic eruption debris
	c) Crystal-lithic, stratified, well sorted, normal graded	Turbidites of reworked volcaniclastic debris
	d) Crystal-lithic, stratified, well sorted, not normal graded	Shallow water, traction sedimented, reworked volcaniclastic debris

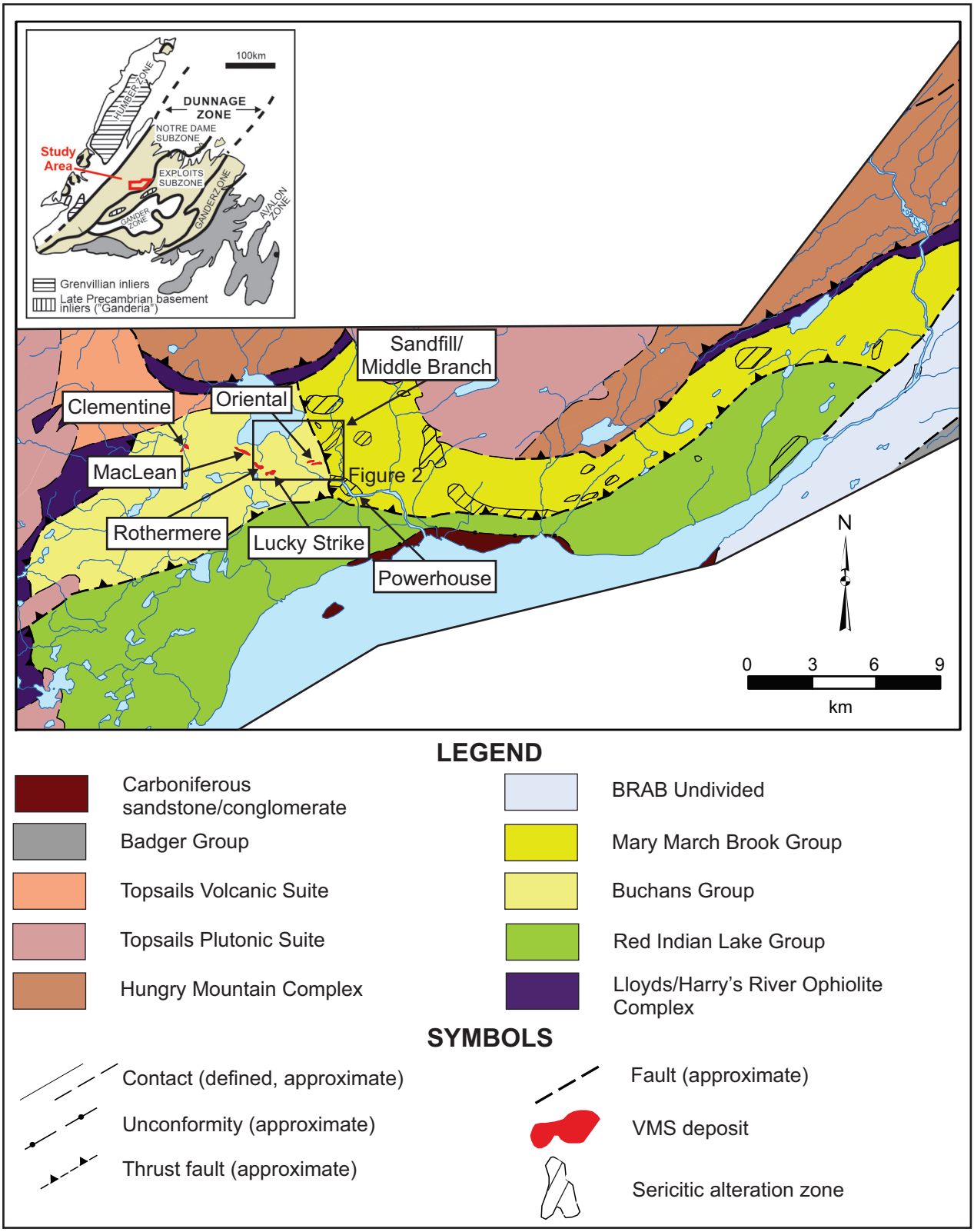

Figure 1. *Regional compilation map outlining the geology and location of select alteration zones relative to the Buchans VMS deposits; geology modified from Zagorevski* et al. *(2015). Note the alteration zones are drawn to encompass drillhole-collar locations that are reported to have intersected sericite alteration at depth; the location of Figure 2 is also shown. BRAB= Buchans–Roberts Arm Belt.*

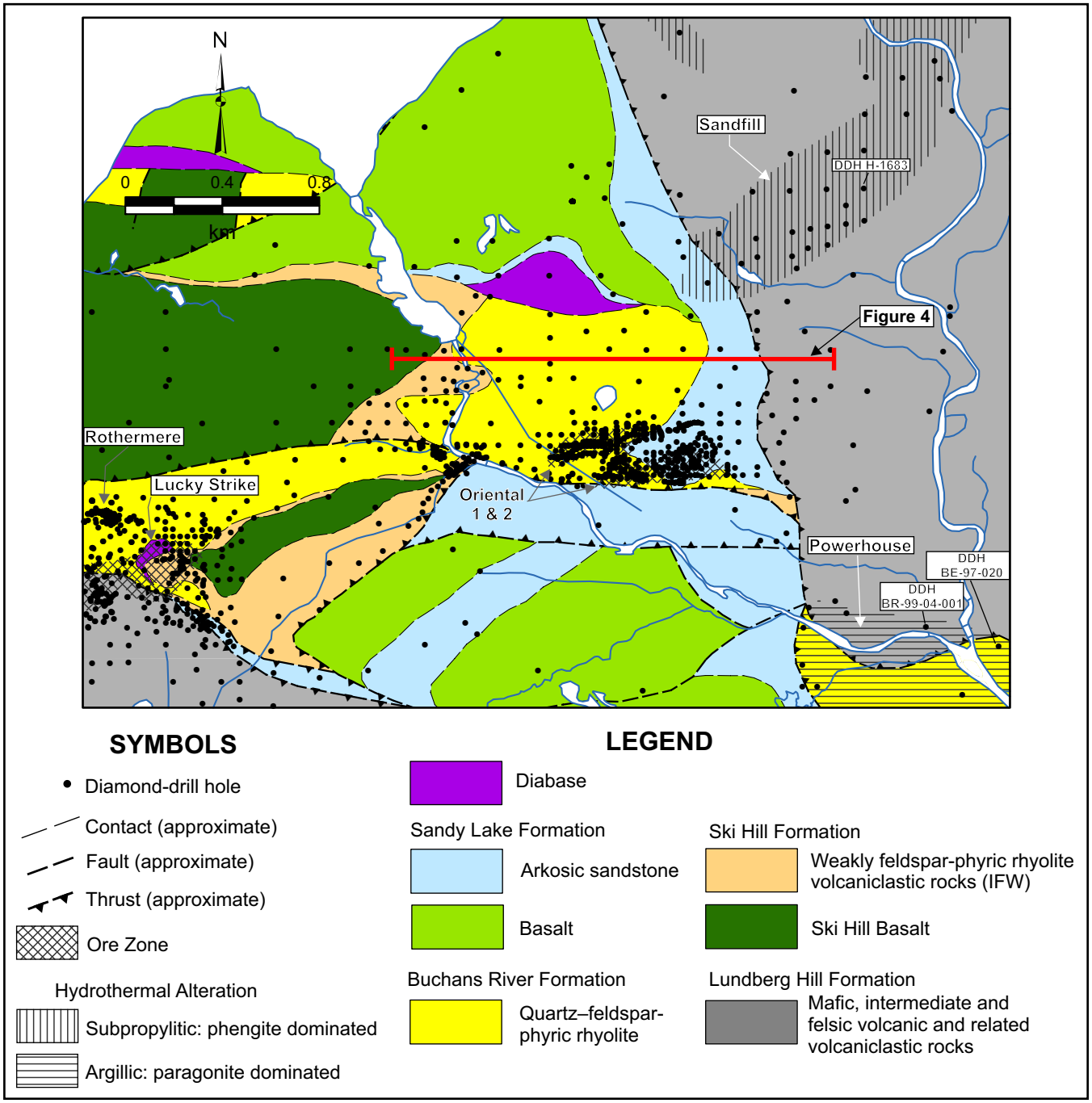

Figure 2. *Local geology map outlining the location of select deposits and prospects within the Buchans area, along with the location of the cross-section shown in Figure 4; modified from Moore and Butler (2019). IFW=Intermediate Footwall member.*

the oldest age in the area of 471 ± 1.6 Ma (Sparkes *et al.*, 2021). Volcanic rocks of *ca.* 470 Ma age are now known to be more widespread than previously thought, with rocks of this age bracketing much of the Buchans Group (*see* Sparkes and Hamilton, *this volume*). The Buchans Group is well known for its VMS mineralization, which includes the past-producing Oriental, Lucky Strike, Rothermere, and MacLean deposits (Figure 1). This VMS mineralization can now be demonstrated to have formed, at least in part, by *ca.* 470 Ma, based on recent geochronological investigations in the area (Sparkes and Hamilton, *this volume*). Rocks correlated with the Buchans Group occur within the footwall of the regionally extensive Airport Thrust fault (Thurlow *et al.*, 1992), and structurally underlie rocks of the Lundberg Hill Formation (Mary March Brook group of Zagorevski and Rogers, 2008, 2009; Figures 1 and 2).

The Mary March Brook group of Zagorevski and Rogers (2008, 2009), which includes elements of the Lundberg Hill Formation, consists of bimodal tholeiitic and calc-alkalic volcanic rocks. The formation of tholeiitic rhyolite cryptodomes and coeval island-arc tholeiitic basalts were accompanied by the deposition of rare polymictic debris flows and locally developed hydrothermal alteration and VMS mineralization, and are conformably overlain by bimodal calc-alkalic volcanic rocks (Zagorevski and Rogers, 2008, 2009). Rocks from within this group are interpreted to have formed within a back-arc or intra-arc rift setting and have been dated using SHRIMP at 461.5 ± 4 Ma (Zagorevski *et al.*, 2015, 2016). However, recent ziron U–Pb dating of the Lundberg Hill Formation has produced a date of 471.7 ± 0.6 Ma (Sparkes and Hamilton, *this volume*), suggesting that some revision of the rocks included within the Mary March Brook group is required.

VOLCANIC FACIES OF THE BUCHANS AREA

In total, eight groups of volcanic facies, containing 16 individual facies, are identified within the Buchans area (Table 2; note the number following the headings listed below relate to the corresponding facies and subclass outlined in the table). Within the immediate Buchans area, the submarine rhyolite dome–cryptodome facies association accounts for the most abundant felsic volcanic facies and can be directly linked with the development of VMS mineralization in the area. The eleven most abundant felsic volcanic facies observed are described below in detail; in approximate decreasing order of abundance, these facies are:

1) Massive monomict vitric breccia with jigsaw-fit (2A).
2) Massive monomict vitric breccia with sedimentary matrix and local jigsaw-fit (2B).
3) Coherent rhyolite (1A).
4) Massive monomict lithic breccia with jigsaw-fit (3A).
5) Massive to diffusely stratified monomict lithic breccia, not jigsaw-fit (3B, 5A).
6) Massive monomict vitric breccia, not jigsaw-fit, matrix to clast supported (2C).
7) Siltstone–sandstone, vitric, diffuse stratified (8A).
8) Siltstone–sandstone, crystal-lithic, stratified, well sorted, normal graded (8C).
9) Massive to stratified polymict lithic breccia–conglomerate, moderate to poorly sorted, clast to matrix supported (7A).
10) Massive to stratified polymict lithic breccia with slurry texture (6E).
11) Welded massive monomict vitric breccia without jigsaw-fit (2D).

COHERENT FACIES (1A)

This facies is abundant in all formations at Buchans. The felsic coherent facies are mainly rhyolitic and weakly to strongly feldspar ± quartz porphyritic (Plate 1). Massive, homogeneous, evenly porphyritic textures with euhedral to subhedral unbroken phenocrysts are most common and provide evidence that these facies are coherent (not clastic). Flow banding, spherulitic texture, lithophysae and perlitic texture occur locally. These facies are interpreted as the coherent cores of lavas and shallow intrusions. In cases where the coherent facies extends all the way to the margin of a unit, it is interpreted as a relatively deep intrusion, emplaced into partly lithified non-water saturated rocks. In cases where the coherent facies grades outwards to hyaloclastite, the unit is interpreted as a lava or shallow intrusion emplaced into water-saturated unlithified strata. Evidence for intrusions include peperitic facies at the contact or similar strata both above and below the unit (*cf.* Allen, 1992).

MASSIVE MONOMICT VITRIC BRECCIA FACIES (2)

Jigsaw-fit (2A)

This facies is characterized by the jigsaw-fit of mainly blocky/equant clasts, abundant curviplanar clast margins and

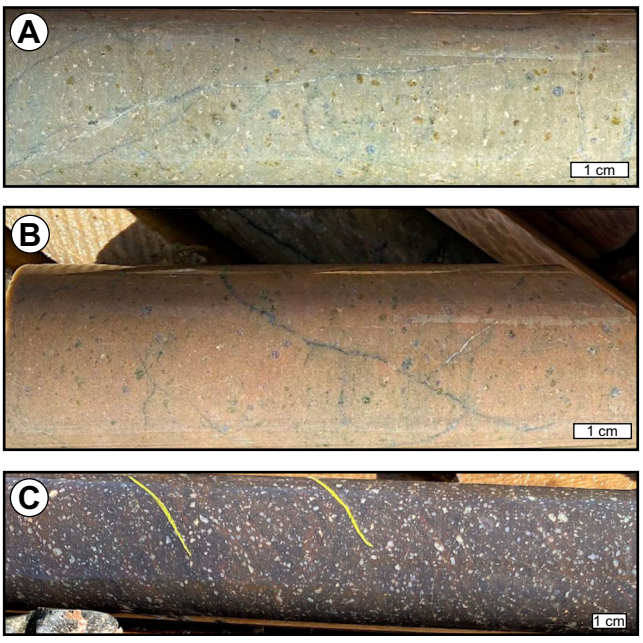

Plate 1. *Coherent felsic facies. A, B) Five percent feldspar> quartz porphyritic coherent rhyolite intrusion, lower Buchans River Formation; DDH H-2228, 238–265 m, Clementine deposit; C) Strongly feldspar–quartz porphyritic coherent rhyolite with faint flow banding, lower Buchans River Formation; DDH H-18-3513, 290 m, Sandfill prospect.*

pervasive mottled sericite–chlorite alteration (Plate 2). The jigsaw-fit arrangement of clasts is commonly subtle and partly obscured by alteration. This texture implies that brecciation/fragmentation occurred *in situ*; *i.e.*, the facies does not comprise transported debris. The abundance of curviplanar clast margins indicates quenching of magma to dense volcanic glass followed rapidly by quench fragmentation of the glass. Quenching occurred by interaction of magma with cold seawater. Locally preserved perlitic fracture texture provides additional evidence of a former glassy (vitric) and dense (non- or weakly pumiceous) composition. The pervasive mottled phyllosilicate-rich alteration is a result of the former glassy character and the inevitable alteration that volcanic glass experiences in the submarine environment, due to diagenetic and/or hydrothermal alteration. This facies generally displays pervasive phyllosilicate-alteration, whereas adjacent non-glassy facies are commonly less altered (*e.g.*, "stoney" felsic intrusions). The genetic term for this *in situ* quench-brecciated facies is "*in situ* hyaloclastite" (*cf.* McPhie *et al.*, 1993). *In situ* hyaloclastite occurs at the margins of subaqueous lavas and shallow intrusions.

Sediment Matrix with Local Jigsaw-fit (2B)

This facies is a variation of the above facies in which the angular curviplanar, formerly glassy, clasts are separated from each other by veins of siliciclastic material, or larger patches of siliciclastic or fine-grained volcaniclastic matrix (Plate 3). The clast aggregate varies from clast- to matrix-supported. The siliciclastic matrix is commonly bleached and moderately silicified, either pervasively throughout, or more commonly in a zoned fashion, comprising pale bleached rims, a few millimetres thick around the hyaloclasts, which grades outward to a darker colour, away from the clasts. The siliciclastic matrix may also locally show soft-state deformed stratification. Local jigsaw-fit clast arrangements combined with the clast shapes indicate *in situ* quench fragmentation, *i.e.*, the facies is hyaloclastite, and the sediment matrix indicates that the hyaloclastite has intruded into soft, wet siliciclastic/volcaniclastic strata. This facies can be termed intrusive hyaloclastite or peperite

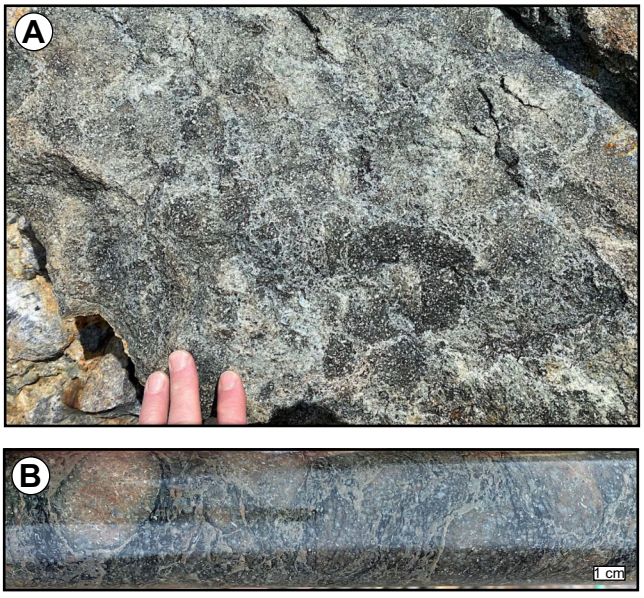

Plate 2. *A) Massive monomict rhyolitic vitric breccia interpreted as* in situ *hyaloclastite. Note jigsaw-puzzle clast arrangement, curviplanar clast margins and mottled alteration; Old Buchans outcrop, lower Buchans River Formation; B) Quartz–feldspar porphyritic, rhyolitic, massive monomict vitric breccia (*in situ *hyaloclastite) showing jigsaw-fit texture and blocky angular clast shapes, lower Buchans River Formation; DDH H-07-3349 181 m.*

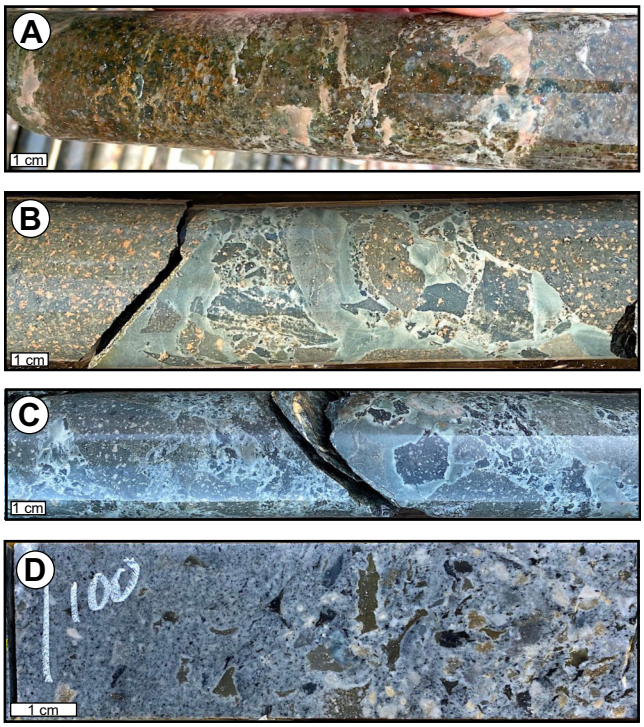

Plate 3. *Massive monomict vitric breccia with sediment matrix, interpreted as intrusive hyaloclastite (peperite). A) Quartz–feldspar-porphyritic rhyolite peperite, lower Buchans River Formation; DDH H-07-3349 124.7 m, Sandfill prospect; B) Feldspar-porphyritic dacitic peperite, Lundberg Hill Formation; DDH H-09-3413 527.2 m, MacLean area; C) Feldspar-porphyritic dacitic peperite, Lundberg Hill Formation; DDH H-09-3413 560 m, MacLean area; D) Massive monomict vitric breccia with sediment matrix interpreted as mud-matrix debris flows that could possibly be locally transported, slumped peperite, Intermediate Footwall member. Note curviplanar-cuspate clast margins, incomplete mixing between mud matrix and clastic aggregate, and normal-graded bed top; DDH H-3356 100 m.*

(McPhie *et al.*, 1993). Such peperites commonly show clusters of jigsaw-fit clasts "frozen" in various stages of disaggregation. Peperite occurs at the intrusive margins of quench brecciated lavas and shallow intrusions and provides evidence that a particular margin is intrusive and not extrusive. Thus, peperite at the upper contact of a unit implies that the unit is an intrusion and not an extrusive flow (Allen, 1992).

Massive to Normally Graded, Matrix to Clast Supported without Jigsaw-fit (2C)

This breccia comprises matrix- to clast-supported aggregates of ragged, equant to elongate flattened, formerly glassy (vitric), vesicular to pumiceous clasts and mainly occurs in units 10s of metres thick (Plate 4). The matrix comprises smaller vesicular clasts or pumice shreds of similar composition to the larger breccia clasts and lesser free (liberated) feldspar and/or quartz crystals. Recognition of clasts, clast boundaries, jigsaw *versus* disorganized texture, and even whether the rock is clastic or not, can be difficult due to the pervasive sericite, chlorite or siliceous alteration that commonly affects these originally pervasive porous glassy facies. Clastic textures are most distinct in breccias that are matrix-supported; the larger vitric clasts are altered to a dark phyllosilicate composition, whereas the matrix has a paler quartz-phyllosilicate composition. This difference is due largely to the control that porosity has on alteration mineralogy and intensity in porous glassy aggregates. Irregular ragged clast margins and internal fibrous textures indicate that the clasts are pumice, and are locally preserved where this facies is least altered or where strong silicification or feldspar-alteration have resulted in a hard competent material that resists deformation. In the more common case, where the rock is pervasively phyllosilicate-altered, the facies can be inferred to be a pumiceous clastic aggregate because of the diffuse characteristic of the clasts; in contrast to dense vitric and lithic clasts, which tend to have more distinct blocky outlines, even where altered. Where the original tops of units are preserved, the breccias show normal grading. The silty-sandy, fine-grained tops of units may contain 2–20 cm irregular shaped lenses of similar composition and porphyritic textured material to that in lower, more massive, parts of the unit. These lenses are interpreted to be large, diagenetically flattened, pumice clasts. Lithic clasts are common, but not essential, and show coarse-tail grading *i.e.*, they become larger and more abundant toward the base of emplacement units.

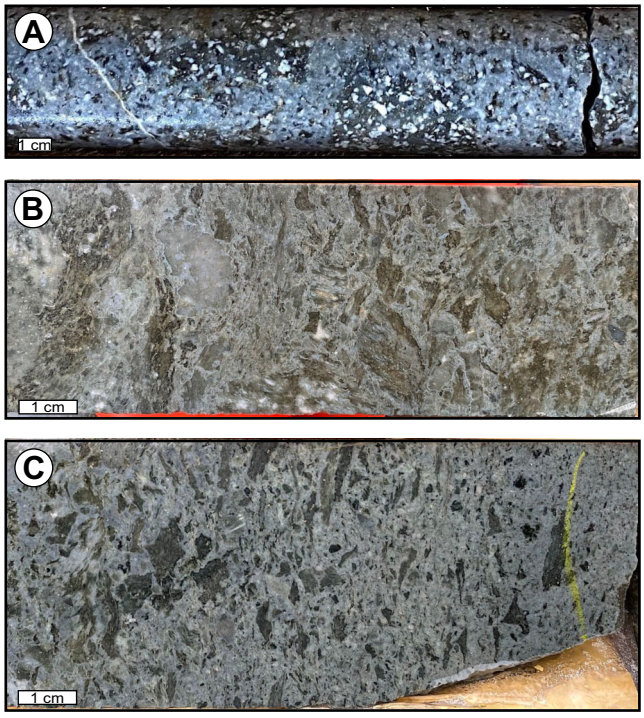

Plate 4. *A) Massive monomict rhyolitic vitric (pumice) ± lithic breccia with 30% quartz–feldspar-phyric, matrix-supported dark sericitic pumice clasts, lower Buchans River Formation; DDH H-1886 213–219 m, Oriental deposit; B) Feldspar-only phyric, moderately–poorly sorted, massive monomict rhyolitic vitric (pumice) ± lithic breccia below the massive sulphide and ore clast horizon, Intermediate Footwall member; DDH H-07-3352 242 m, Oriental deposit; C) Features of the top of a pumice breccia bed, Intermediate Footwall member. Note the normal grading; DDH H-07-3352 240 m, Oriental deposit.*

The monomict pumice-rich character suggests that this facies was sourced directly from magmatic pyroclastic eruptions. Units with more blocky, less pumiceous clasts, could be derived from phreatomagmatic pyroclastic eruption or from the gravitational collapse of the flanks of lava domes. The bedform of a massive lower part, and a normal-graded top implies that the debris was transported as a subaqueous clastic mass flow (essentially a megaturbidite) in deep water (below wave base). The large pumice clasts in the fine-grained graded bed tops represent pumice clasts that initially floated and then became waterlogged, and settled at the same time as the fine-grained ash of the uppermost part of the mass-flow deposit.

Welded Massive Monomict Vitric Breccia without Jigsaw-fit (2D)

This facies is similar to the 2C facies described above, except that the units do not have normal-graded tops and locally there is evidence that the clastic pumice aggregate was hot enough to weld together upon deposition. Evidence for welding comprises eutaxitic texture in the matrix and within large pumice clasts (fiamme), and perlitic fracture texture (Plate 5). Eutaxitic texture comprises millimetre-scale fluidal-shaped lenses having a strong preferred align-

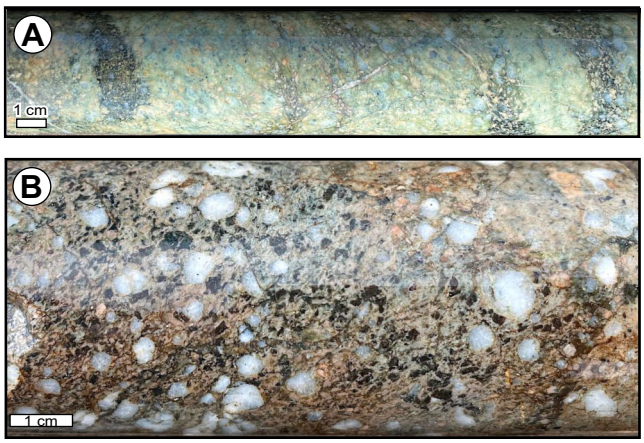

Plate 5. *Welded massive monomict vitric (± lithic) breccia without jigsaw-fit (2D) facies within the prominent quartz unit of the Lundberg Hill Formation. A) Drillcore from northwest of MacLean, showing welded massive monomict matrix-supported rhyolitic pumice (vitric) breccia with dark lenses that represent large welded pumice clasts (fiamme); DDH H-09-3413 975–980 m; B) Drillcore from the Engine House area showing perlitic fracture texture in the matrix; DDH H-3447 2–14 m.*

ment. These micro lenses are flattened glass shards welded together and the walls of vesicles compressed and welded together. Perlitic texture comprises arcuate-ovoid fractures formed during hydration of glass and implies that after welding, the rock was a dense glass. Welding is extremely rare in subaqueous pyroclastic deposits however, it is common in thick, subaerial pyroclastic deposits. Therefore, it is most likely that the welded facies is a subaerial pyroclastic flow deposit.

MASSIVE MONOMICT LITHIC BRECCIA FACIES (3)

Jigsaw Textured (3A)

This facies is characterized by monomict lithic breccia hosting abundant jigsaw-fit clasts, which are cemented by hydrothermal quartz ± sulphides or locally by other hydrothermal minerals such as barite or carbonate ± sulphides (Plate 6). Such breccias are commonly hosted within moderately to strongly silicified or quartz-sericite altered units. The fracture pattern comprises planar to sinuous to serrated fractures having a paucity of the curviplanar/broad cuspate fractures that characterize hyaloclastite. The breccias range from close-packed entirely jigsaw-fit clast arrangement to disorganized (minor jigsaw-fit) more open framework clast- to almost matrix-supported breccia in which clasts have been rotated and perhaps even transported some distance within the breccia. Accompanying this variation from close-packed jigsaw-fit to more matrix-rich clast

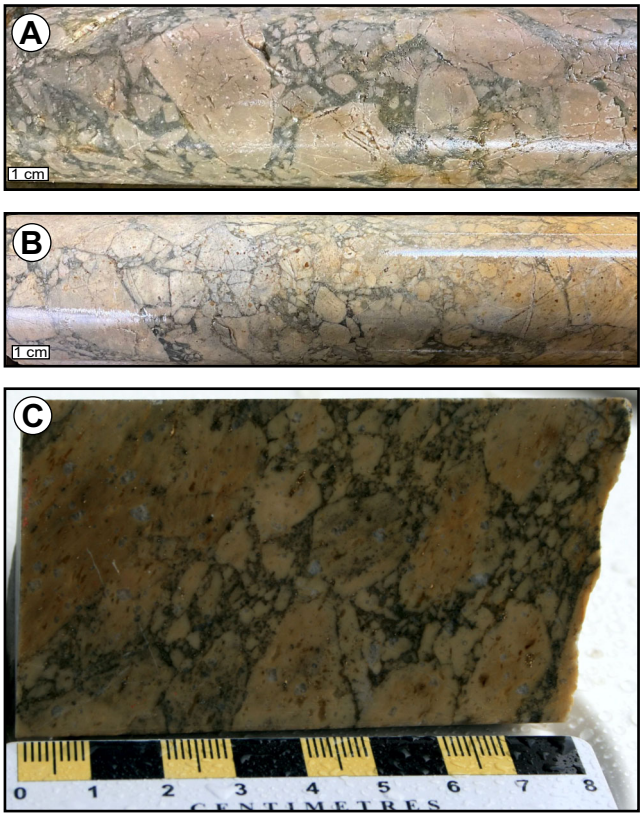

Plate 6. *Massive monomict lithic breccia facies interpreted as* in situ *hydrothermal breccia in weakly feldspar>quartz-porphyritic rhyolite. Note planar to sinuous fractures and clast margins, and subrounding of some clasts in more matrix rich areas. A) Disorganized hydrothermal breccia; DDH H-09-3410 54 m, Clementine deposit; B) DDH H-09-3410 41–48 m, Clementine deposit; C) DDH BE-97-020 103 m, Powerhouse prospect.*

arrangement, the clast shapes vary from very angular blocky and wedge-shaped, to subrounded equant and crudely triangular, respectively. In detail, the rounding is not smooth as in sedimentary rounding, but rather comprises numerous tiny cuspate segments that result in a subrounded finely serrated margin. Some major through-going fractures in a particular orientation are commonly present, however these may be difficult to recognize in drillcore; fractures that cut earlier cemented fractures also occur. Fracture patterns, clast shapes and ubiquitous hydrothermal alteration and cement are characteristic features of hydrothermal breccia. The variants with moderate to abundant jigsaw-fit clast organization are defined as "*in situ* hydrothermal breccia" and the variants with disorganized clast arrangement are defined as "disorganized hydrothermal breccia". With increasing disorganization and amount of matrix, due to increased clast transport, the disorganized hydrothermal breccias become hydrothermal breccia dykes (or sills).

STRATIFIED MONOMICT LITHIC BRECCIA FACIES (5)

Polychromatic (5A)

This facies comprises moderately to locally well-sorted, clast-supported aggregates of monomict to weakly polymict, lithic (stoney crystalline rather than glassy) rhyolite lava clasts (Plate 7). A subordinate component of basalt clasts is common and massive sulphide clasts occur locally (*e.g.*, Sandfill prospect). The rhyolite clasts typically range from blocky- to slabby- to wedge-shaped and are angular to subrounded within the same unit. The clasts are either pervasively bleached and/or silicified, or show variable colour due to variation in the intensity and mineralogy of alteration from clast to clast and even within individual clasts, imparting a superficially polymict appearance to the rock. Although some clasts appear rounded, in detail the rounding is not smooth as in sedimentary rounding, rather comprises numerous tiny cuspate segments that result in a subrounded finely serrated margin. This style of subround, serrated clast shape is attributed partly to the sinuous-serrated form of the fractures that define the clast margins and partly to violent clast collisions that cause chips to be knocked off the margins of the clasts. Some parts of these, more stratified intervals, contain successions of normal-graded beds, which indicate deposition from turbidite mass flows in deep water. However, other parts within the same unit of lithic breccia–

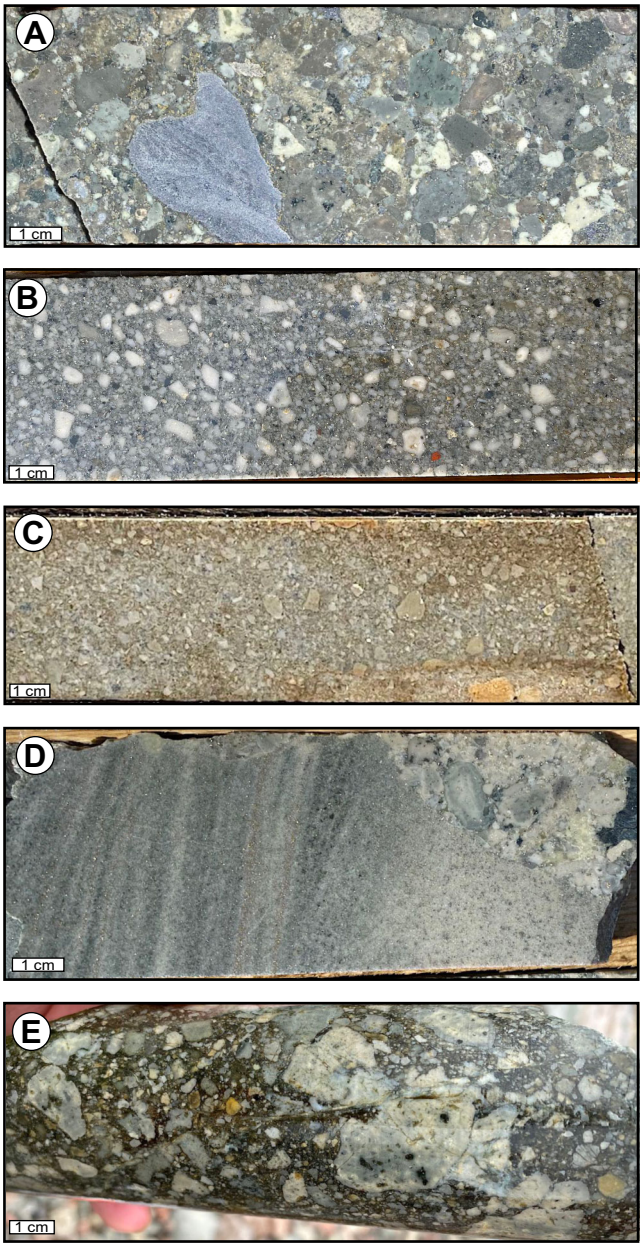

Plate 7. *A) Massive to diffusely stratified, clast-supported, polychromatic, weakly polymict, rhyolitic lithic breccia facies interpreted as hydrothermal eruption breccia. Clasts are mainly weakly feldspar>quartz(<1%)-porphyritic rhyolite and minor basalt and quartz–feldspar-porphyritic rhyolite. Massive sulphide and barite clasts are locally abundant, Intermediate Footwall member; DDH H-18-3513 351 m, Sandfill prospect; B) Massive to diffusely stratified, matrix-supported, polychromatic, weakly polymict, rhyolitic lithic breccia facies, interpreted as hydrothermal eruption breccia, lower Buchans River Formation. Clasts are weakly feldspar>quartz(<1%)-porphyritic rhyolite. Note some subrounded clast shapes, diffuse stratification, strong alteration of clasts (silicification + pyrite), strong disseminated pyrite in matrix, and variable colour due to variation in intensity and mineralogy of alteration both among clasts and within individual clasts; DDH H-09-3410 210 m, Clementine deposit; C) Massive to diffusely stratified, clast-supported, moderately–poorly sorted, polychromatic, monomict, rhyolitic lithic breccia facies, interpreted as hydrothermal eruption breccia, lower Buchans River Formation. Clasts are weakly feldspar>quartz(<1%)-porphyritic rhyolite, strongly silicified and with pervasive quartz-pyrite altered matrix. Note: blocky to wedge and shard shaped clasts and some subrounded clasts; DDH H-09-3410 202–210 m, Clementine deposit; D) Stratified, clast-supported, monomict to weakly polymict, rhyolitic lithic breccia–sandstone facies, interpreted as hydrothermal eruption breccia, Intermediate Footwall member. Note scour at base of breccia bed on crossbedded sandstone; DDH H-3513 356 m, Sandfill prospect; E) Diffusely stratified, matrix-supported, polychromatic, weakly polymict, rhyolitic lithic breccia facies interpreted as hydrothermal breccia, Intermediate Footwall member; DDH H-07-3349 340 m, Sandfill prospect.*

sandstone may show scours, crossbedding, reverse graded gravel layers and gravel lag horizons, which imply traction sedimentation.

The clast shapes, the monomict lithic composition and the generally strong alteration, suggest that this facies resulted from hydrothermal brecciation. The moderate to good sorting, local stratification and associated stratified gravelly sandstone, indicate that the clastic aggregate was transported laterally, and deposited by traction sedimentation. This facies is attributed to violent hydrothermal eruptions within rhyolite lava domes and cryptodomes (shallow intrusive domes). Numerous repeated hydrothermal eruptions resulted in a thick clastic talus apron of hydrothermal eruption breccia on the flank of, and adjacent to, the lava dome or cryptodome.

MASSIVE TO STRATIFIED POLYMICT LITHIC BRECCIA FACIES (6)

Slurry Texture (6E)

Massive to diffuse stratified, monomict to polymict lithic breccia with "slurry texture" (matrix-rich and very poor sorting) and sharp intrusive contacts occurs in many drill-cores at Buchans (Plate 8). The units range from 10 cm to several metres thick. They occur within coherent lavas/intrusions, along rock unit contacts and within fault zones or along inferred fault contacts. They are dominated by volcanic clasts, but may also contain granite, massive sulphide and barite clasts. Clasts mainly have the shapes and characteristics described above for the "massive monomict lithic breccia with jigsaw-fit (3A)" and "massive to diffusely stratified, monomict to slightly polymict, lithic breccia (5A)" facies that are interpreted as hydrothermal breccia and hydrothermal eruption breccia, respectively. These characteristics, the locations of the breccias, and the sharp contacts, suggest that this facies includes synvolcanic hydrothermal breccia dykes ± sills related to over-pressured hydrothermal solutions and also hydraulic breccia dykes ± sills formed by brecciation and release of over-pressured fluids along fault zones and thrust planes during deformation.

Plate 8. *Massive poorly-sorted, matrix-supported breccia facies interpreted as breccia dykes; note the very poorly-sorted "slurry textured" of the polymict lithic breccia; DDH H-3410 320 m, Clementine deposit.*

MASSIVE TO STRATIFIED POLYMICT LITHIC BRECCIA–CONGLOMERATE FACIES (7)

Moderately- to Poorly-sorted, Clast- to Matrix-supported Breccia–Conglomerate (7A)

Although not volumetrically abundant, this facies is relatively common and widespread (Plate 9). In the Buchans River Formation, some of the breccia–conglomerates contain massive sulphide and/or barite clasts and locally constitute ore bodies. The facies comprises moderately to poorly sorted, clast-supported to locally matrix-supported coarse breccias and breccia–conglomerates, which in several cases, grade upward into successions of interbedded breccia and normal-graded gravelly sandstone. The breccia–conglomerates are distinguished in having a mixture of angular blocks as well as some well-rounded cobbles. Some units are composed entirely of volcanic clasts, whereas others have a component of granite and/or diorite clasts. The granite and diorite clasts are almost invariably rounded to some degree and commonly more rounded than the accompanying volcanic clasts. Although most facies characteristics of these breccias are independent of the clast compositions, it is useful to subdivide the facies according to whether they contain granite–diorite clasts and/or massive sulphide-barite clasts. The massive, moderately to poorly sorted, clast-supported arrangement and locally preserved normal-graded tops, indicate deposition from subaqueous granular, high-clast concentration mass flows. The well-rounded granite and diorite clasts imply reworking in a river or beach environment, prior to re-sedimentation into the deep water part of the basin. Re-sedimentation into the deeper water site of massive sulphide formation, amongst locally derived juvenile volcanic facies, suggest that the breccias and breccia–conglomerates with granite–diorite clasts represent the distal tongues of fan-deltas that shed polymict debris into the basin from basin margin fault scarps.

SILTSTONE–SANDSTONE FACIES (8)

Vitric, Diffuse Stratified (8A)

This facies is commonly pale grey and homogeneous, with local normal-graded tuffaceous sandstone beds and thin layers of ragged pumice clasts (Plate 10A, B). The facies may contain scattered crystal fragments, but is not crystal-

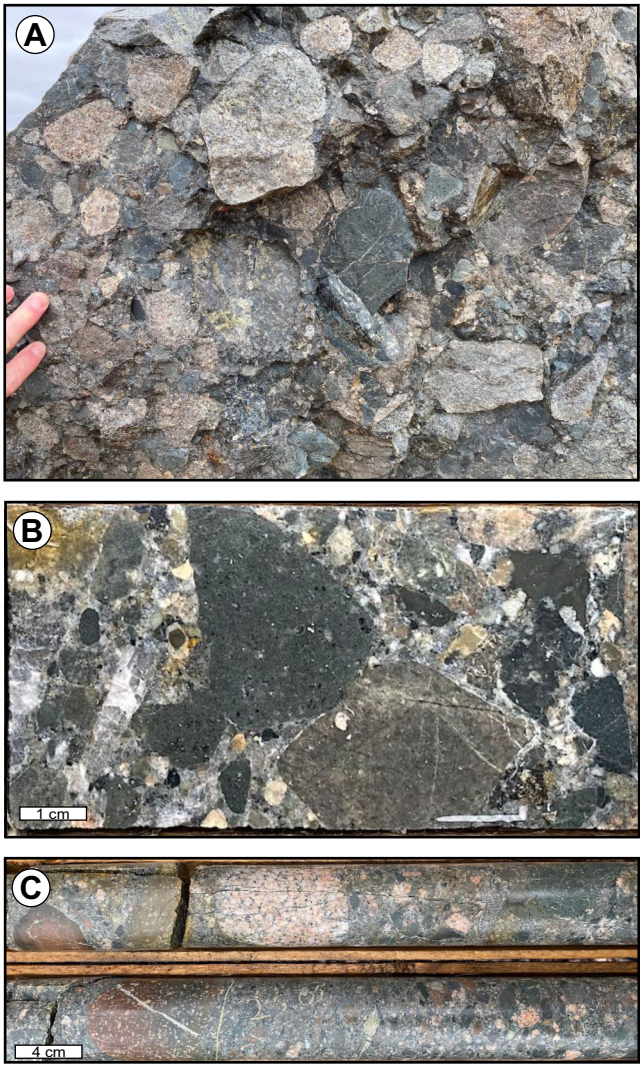

Plate 9. *Massive, poorly-sorted, polymict lithic breccia–conglomerate with granite and ore clasts. Note rounding, especially of the abundant granite clasts. Interpreted as mass flow deposits of reworked volcanic and granite debris, shed into the basin from an adjacent shallow-marine or fluvial environment. A) Lower Buchans River Formation, Old Buchans outcrop; B) DDH H-08-3369A 20–30 m, Buchans River Formation, Lucky Strike deposit; C) Massive, poorly-sorted, polymict lithic breccia–conglomerate with granite clasts that has distinct gravel to sand grain size normal-graded top, Buchans River Formation; DDH BR-2K-01-04 20.5–26.8 m, Sandfill prospect.*

rich. The paucity of crystals implies that the facies is mainly composed of tiny volcanic glass particles, probably glass shards and pumice shreds. This facies is attributed to medial–distal subaqueous fallout and turbidity current deposits, derived from pyroclastic and hydrothermal eruptions at lava dome vents.

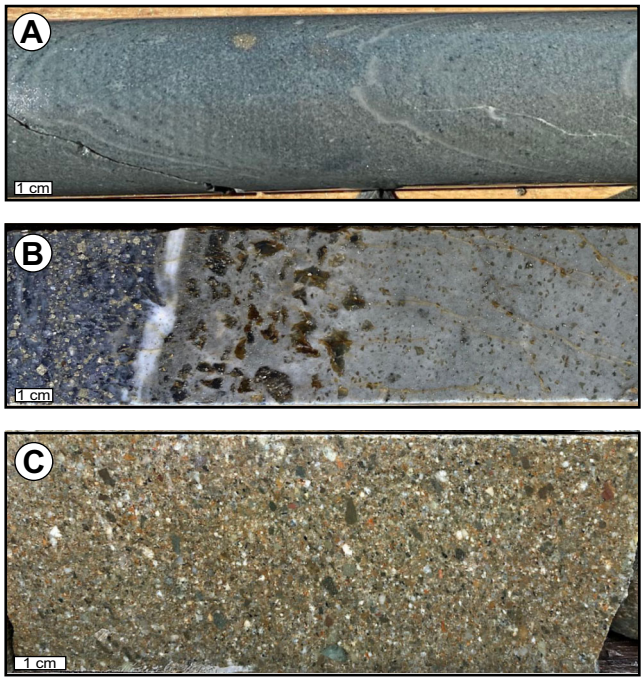

Plate 10. *Siltstone–sandstone facies. A) Diffuse stratified, tuffaceous siltstone–sandstone, Intermediate Footwall member, DDH H-18-3500 68 m, Lucky Strike deposit; B) Normal-graded thin pumice and ash bed within vitric siltstone–sandstone, Intermediate Footwall member. Note the strong sericite–pyrite alteration; DDH H-3356 41 m, Lucky Strike deposit; C) Moderately sorted, crystal-lithic sandstone, Sandy Lake Formation; DDH H-07-3352 337–347 m, Oriental deposit.*

Crystal-lithic, Stratified, Well Sorted, Normal Graded (8C)

Stratified, crystal-lithic, volcanic sandstone–siltstone facies comprises successions of well-sorted, normal-graded beds up to 10s m thick and is the most characteristic facies of the Sandy Lake Formation (Plate 10C). The non-pumiceous, non-juvenile, crystal ± lithic-rich composition indicates that this facies was derived from the reworking of, and concentration of crystals ± lithics, from other volcanic facies; most likely pyroclastic deposits. The extreme concentration of crystals ± lithics implies reworking in a traction current regime, either river or shallow-marine environment, whereas the normal-graded bedforms imply final transport and deposition from turbidity currents below wave base.

LOCAL GEOLOGY OF THE BUCHANS AREA

The stratigraphy of the Buchans area has recently been modified by Allen and Schofield (2023) from that originally

proposed by Thurlow and Swanson (1987). This revised stratigraphy is summarized in Table 3 and illustrated in Figure 3. Modifications to the lithostratigraphic nomenclature include the introduction of three new members into the Buchans River Formation (Buchans Camp, Clementine and Oriental-Sandfill members), which are informally grouped into an upper (Buchans Camp member) and lower (Clementine and Oriental-Sandfill members) Buchans River Formation, in addition to the re-instatement of the Intermediate Footwall unit of Thurlow and Swanson (1981) now as a member within the Ski Hill Formation. Most of these units formed *ca.* 470 Ma and are inseparable within existing geochronological constraints (*cf.* Sparkes and Hamilton, *this volume*). Note that work by Allen and Schofield (2023) also supports the inclusion of the Woodmans Brook volcanic rocks of Winter (2000) and Thurlow (2001) (those rocks occurring immediately east and within the hangingwall of the Airport Thrust fault; Mary March Brook group of Zagorevski *et al.*, 2015; Figure 1) within the existing Lundberg Hill Formation (*see* below). Only the felsic-dominated facies are discussed here, as they are most relevant to the development of VMS mineralization.

Table 3. Modified stratigraphic nomenclature of the Buchans area. Note units arranged in stratigraphic order from top to bottom

Group	Formation	Member
Buchans	Sandy Lake	
	Buchans River	Buchans Camp
		Clementine
		Oriental-Sandfill
	Ski Hill	Intermediate Footwall
		Ski Hill
	Lundberg Hill	

The felsic-volcanic facies occur within the Intermediate Footwall member and comprise almost the entirety of the Buchans River Formation. The submarine rhyolite dome–

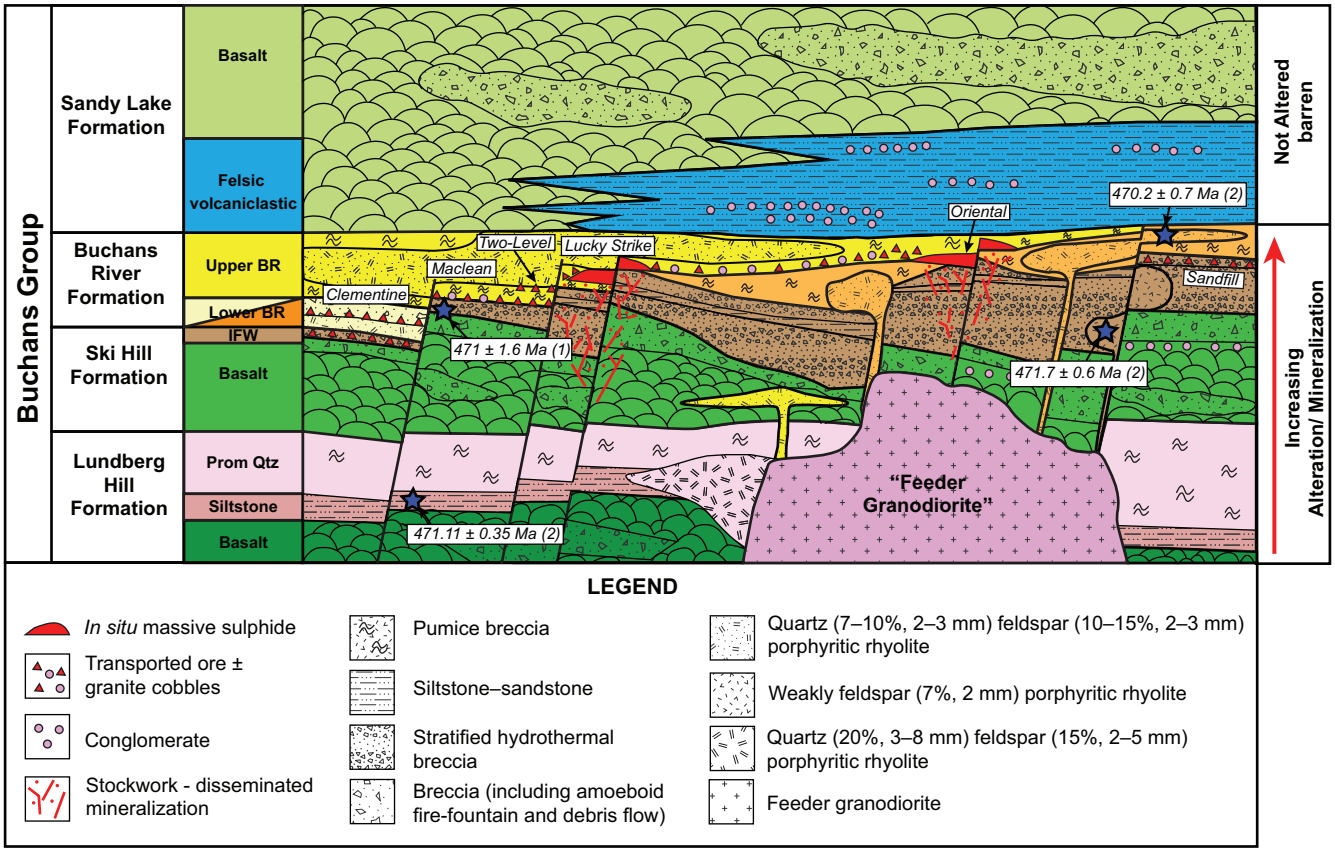

Figure 3. *Revised stratigraphic scheme for the Buchans area (modified from Allen and Schofield, 2023; modified from Thurlow and Swanson, 1987). Note the numbers following the compiled geochronology samples (blue stars) represent the data source: (1) Sparkes* et al.*, 2021; (2) Sparkes and Hamilton (*this volume*). Prom Qtz=Prominent quartz unit; IFW=Intermediate Footwall member of the Ski Hill Formation, Upper BR=Upper Buchans River (Buchans Camp member), Lower BR=Lower Buchans River, and the division of the lower Buchans River Formation illustrates the Clementine (light yellow) and Oriental-Sandfill (orange) members.*

cryptodome facies association forms thick tabular units with a crudely concentric distribution of component facies. In general, the facies range from an outer domain of massive to normal graded, monomict vitric (± lithic) breccia facies without jigsaw-fit (2C) with gradational or sharp contacts inwards with heterogenous mottled-altered, massive monomict vitric breccia with jigsaw-fit (2A) that, in turn, locally grades inwards to coherent rhyolite (1A; Figure 4). The outer pumice breccia, the hyaloclastite and the coherent rhyolite have in most cases similar phenocryst populations (size and abundance) and immobile element ratios. In several cases, a thick tabular (?) lens of weakly altered brown "stoney" coherent rhyolite with sharp contacts occurs in the core of the facies association.

This association of rhyolite facies represents the classic eruptive cycle of a rhyolite dome volcano, comprising pyroclastic eruption of initial gas-rich (pumiceous) rhyolite magma, followed by passive intrusion of the remaining degassed magma into the pyroclastic deposit (*cf.* Cole, 1970). The thick, massive to normal-graded bedforms indicate that the pumice breccia facies was deposited in deep water (below wave base) from subaqueous mass flows. The degassed magma that intruded the pyroclastic deposit became extensively quenched to hyaloclastite breccia because of the subaqueous environment. The similar physical and chemical composition of the pumice breccia, hyaloclastite and local coherent rhyolite indicate that these facies were emplaced during the same eruption from the same pulse of magma. In contrast, the "stoney" rhyolite that occurs in the core of the facies association was not quenched, is less altered and probably represents an intrusion into the dome volcano by a slightly younger pulse of rhyolite magma with a slightly different phenocryst population but similar chemical composition.

ORE HORIZONS

Two camp-wide and three additional, local, ore horizons are distinguished in the Buchans area. These ore horizons occur in association with the emplacement of four separate rhyolite dome–cryptodome eruption packages (*see* below; Figure 3). The extent and style of mineralization of these ore horizons, in stratigraphic order from top to bottom, are:

1) Near the base of the Buchans Camp member of the upper Buchans River Formation; this represents a local ore horizon that hosts *in situ* massive sulphide at the Lucky Strike deposit, and transported ores at MacLean and MacLean Extension deposits.
2) At or near the top of the Clementine member of the lower Buchans River Formation, south of the Clementine deposit. Combined with the ore horizon at the top of the Oriental-Sandfill member, this becomes a camp-wide horizon at the top of the lower Buchans River Formation.

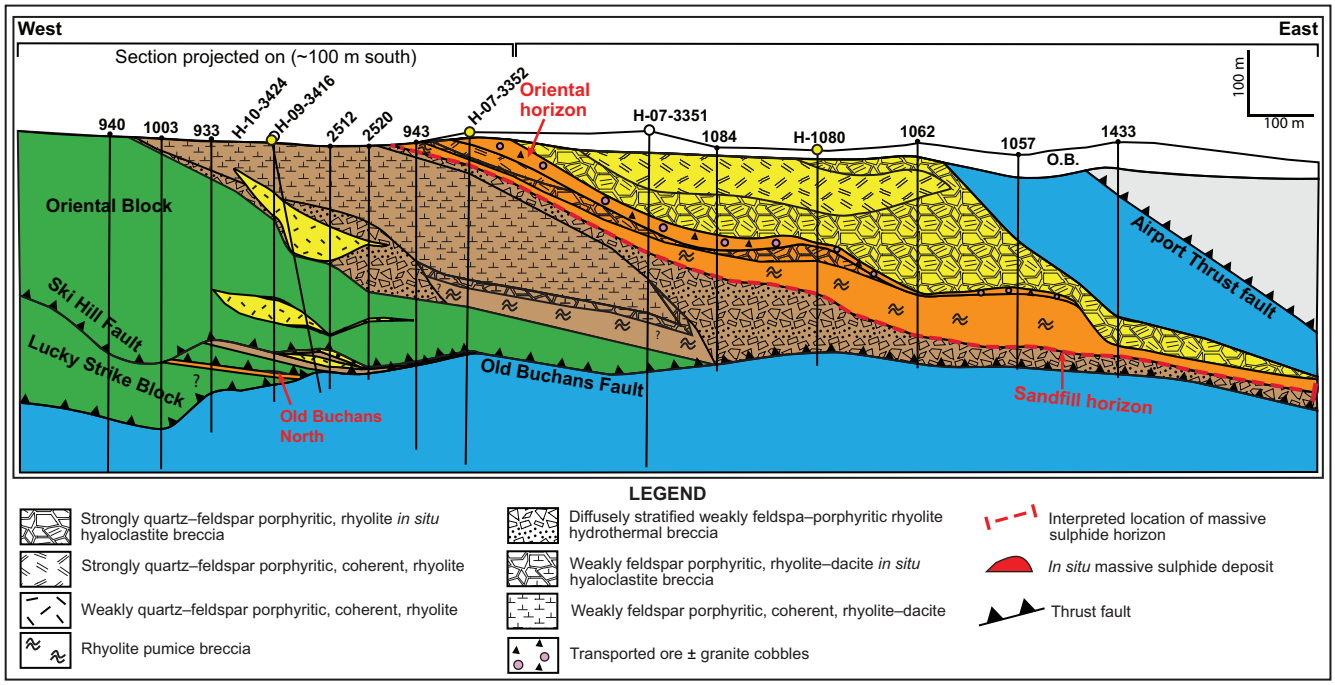

Figure 4. *Cross section through the area of Old Buchans North and Sandfill prospects (from Allen and Schofield, 2023). Note the colour of units follow that defined in Figure 3.*

3) Middle of the Clementine member of the lower Buchans River Formation at the Clementine deposit; this represents transported ore-clast breccia.
4) Top of the Oriental-Sandfill member of the lower Buchans River Formation in the Oriental-Sandfill area; hosts the Oriental 2 transported ore-clast breccia, in addition to ore- and granite-clast breccia–conglomerate north of Oriental.
5) Top of the Intermediate Footwall member of the Ski Hill Formation throughout the Buchans Camp; hosts the Oriental 1 ore-clast breccia, the transported ore-clast horizon at the Sandfill prospect, and the lower transported ore-clast horizon at the Clementine deposit.

The stratigraphic thickness of the lava domes, cryptodomes, sills and pumiceous mass-flow units between ore horizons is up to 190 m. All of these facies were rapidly emplaced and the time interval that elapsed between the ore horizons may be short. The stratigraphic position of these ore horizons emphasizes the significance of the division of the Buchans River Formation into members, and the reinstatement of the Intermediate footwall unit of Thurlow and Swanson (1981) as a distinct member of the Ski Hill formation.

GEOCHEMISTRY

Using immobile element lithogeochemistry, the volcanic rocks within the Buchans area are subdivided into five magmatic affinities ranging from tholeiitic to calc-alkaline (Figure 5A), and eleven volcanic divisions, comprising 4 rhyolitic, 1 dacitic, 1 andesitic–dacitic and 5 basaltic units (Figure 5B). The ratios Th/Yb and Zr/Y are most useful in distinguishing magmatic affinity, and Zr/Al_2O_3 and Al_2O_3/TiO_2 are most useful in distinguishing the various volcanic compositions.

Barrett (2012) used ratios of immobile elements to subdivide volcanic rocks at Buchans into various magmatic affinity groups. Allen and Schofield (2023) built on this previous work and applied the concept to a larger database of lithogeochemical data. The main divisions of magmatic affinity (magma series) are tholeiitic and calc-alkaline with volcanic rocks displaying characteristics between the tholeiitic and calc-alkaline series being referred to as "transitional". In total, two groups of calc-alkaline affinity, two of transitional affinity and one of tholeiitic affinity can be identified (Figure 5A). At Buchans, magmatic affinity is very useful in discriminating the various stratigraphic formations and also in discriminating the rhyolitic host rocks associated with mineralization.

Rhyolitic rocks form the immediate footwall to VMS mineralization (Intermediate Footwall member and locally the Buchans River Formation) as well as the hangingwall (Buchans River Formation). Consideration of volcanic facies type, stratigraphic position relative to mineralized horizons, along with immobile element ratios of these units, shows that some identical looking rock units have distinctly different immobile element ratios, and also the converse, that some rock units that have very different phenocryst populations have more or less identical ratios between Zr, TiO_2 and Al_2O_3. However, by using a combination of volcanic-facies characteristics including the amount and type of phenocrysts, the volcanic composition from Zr/Al_2O_3 and Al_2O_3/TiO_2 ratios, and magmatic affinity especially from the Th/Yb ratio, all rhyolitic units that underlie, separate and overlie the various VMS ore horizons can be distinguished and correlated.

At the large scale, the data indicates that the lower part of the succession, the Lundberg Hill and Ski Hill formations (excluding the Intermediate Footwall member), contain abundant basalt and andesite and a moderate amount of rhyolite. The overlying Intermediate Footwall member and Buchans River Formation are dominantly rhyolitic with only minor mafic and andesitic–dacitic rocks. Consequently, the Lundberg Hill and Ski Hill formations can be regarded as bimodal, whereas the Intermediate Footwall member and Buchans River Formation are not on their own bimodal. The Sandy Lake Formation at the top of the succession appears to be strongly bimodal having abundant rhyolite and basalt and a marked paucity of andesite.

Mafic rocks in the Lundberg Hill Formation are tholeiitic, whereas mafic rocks in the overlying Ski Hill and Sandy Lake formations are transitional, which suggests a progression in time to more evolved mafic magmas. Although the Lundberg Hill Formation contains a component of calc-alkaline felsic rocks, the Intermediate Footwall member, Oriental-Sandfill member, Clementine member, Buchans Camp member and Sandy Lake Formation, show a progression from transitional through intermediate transitional-calc-alkaline to calc-alkaline characteristics, which also suggests an evolution with time to more evolved felsic magmatic compositions.

Lundberg Hill Formation

Facies within this formation indicate widespread felsic and mafic volcanism in a mixed subaerial and submarine environment. The Lundberg Hill Formation and Woodmans Brook volcanic rocks of Thurlow (2001) have remarkably similar volcanic facies, volcanic compositions and magmatic affinity and are therefore interpreted as structural repetitions of the same formation. In particular, the Lundberg Hill Formation and Woodmans Brook volcanic rocks are both dominated by tholeiitic and calc-alkaline-2 affinity, unlike

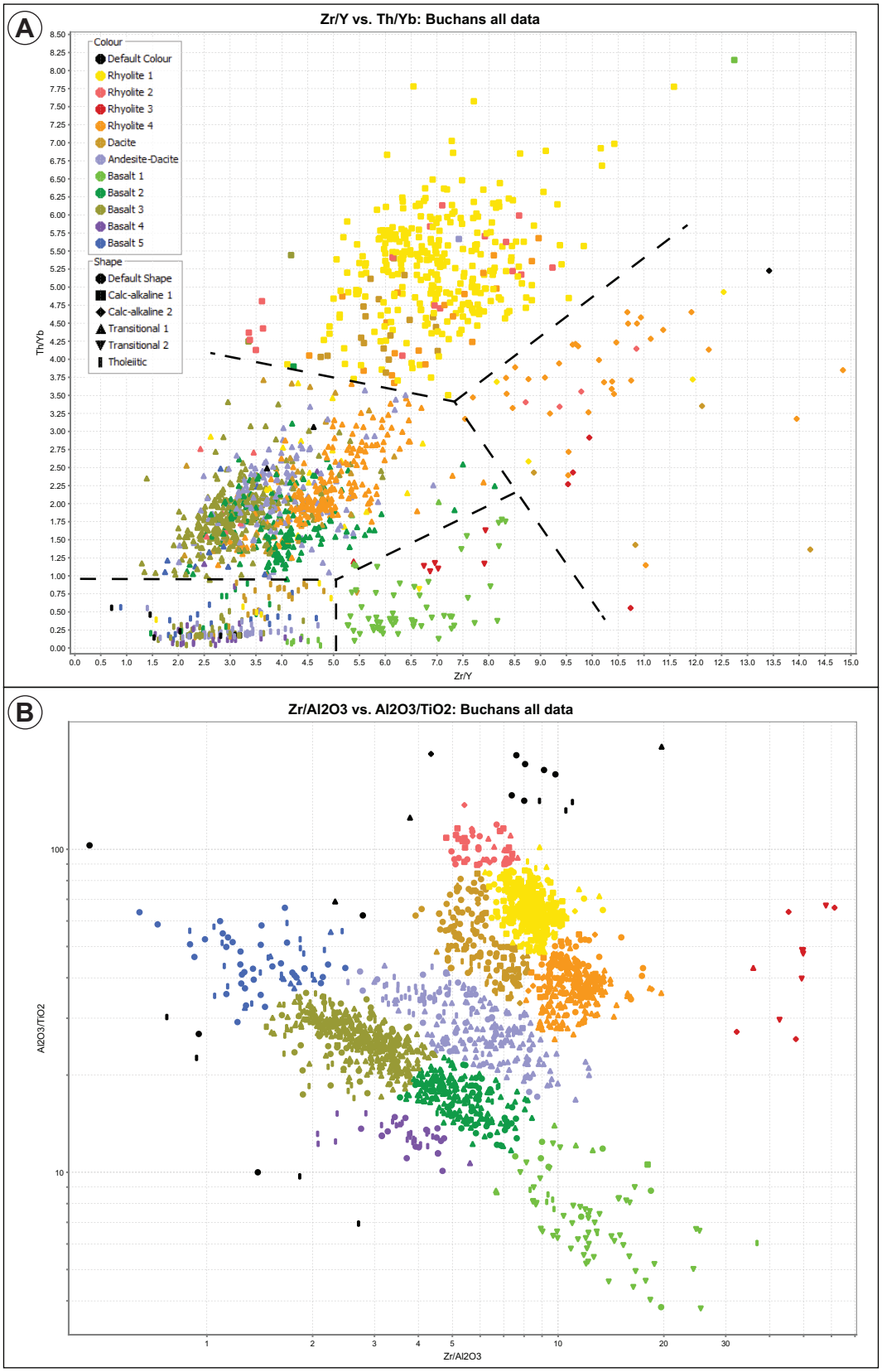

Figure 5. *A) Zr/Y* vs. *Th/Yb plot showing the volcanic compositions versus magmatic affinity for the Buchans area (from Allen and Schofield, 2023; modified after Barrett, 2012); B) Zr/Al2$_2$O$_3$* vs. *Al$_2$O$_3$/TiO$_2$ plot outlining the subdivisions of volcanic compositions for the Buchans area (from Allen and Schofield, 2023).*

any other formation (Figure 5A). Rhyolite-4 of calc-alkaline-2 affinity is common in both the Lundberg Hill Formation and Woodmans Brook volcanic rocks and does not occur in any other formation. These rocks include the "prominent quartz" pyroclastic flow deposits. Most of the mafic volcanic rocks grouped within the basalt-5 subdivision also primarily occur within the Lundberg Hill and Woodmans Brook volcanic rocks (Figure 5A, B); these comprise fire fountain breccias, pillow lava, volcaniclastic rocks and intrusions. Furthermore, the Lundberg Hill and Woodmans Brook volcanic rocks are the only formations that have rocks of tholeiitic composition. Although the Lundberg Hill and Ski Hill formations both have abundant basalt-3 and andesite–dacite, those in the Lundberg Hill Formation are tholeiitic, whereas those in the Ski Hill Formation are of transitional-1 affinity (*i.e.*, they are not formed from the same magmas; Figure 5A, B).

Ski Hill Formation

The Ski Hill member of the Ski Hill Formation represents a period of extensive submarine mafic volcanism, which preceded emplacement of the submarine rhyolite domes of the Intermediate Footwall member and the Buchans River Formation, that are associated with VMS mineralization. The Ski Hill Formation is characterized by abundant basalt-3 and andesite–dacite, and minor basalt-2 and rhyolite-4, all of transitional-1 affinity (whereas in the Lundberg Hill Formation basalt-3 and andesite–dacite are tholeiitic; Figure 5A, B). The true stratigraphic component of the Ski Hill Formation consists almost entirely of transitional-1 affinity. The mafic rocks of Ski Hill Formation include pillow lava, fire fountain bomb and breccia deposits, sheet lava, and re-sedimented mafic volcaniclastic deposits derived via collapse and lateral transport of debris from the *in situ* deposits, and various mafic intrusions. The Intermediate Footwall member portion of the Ski Hill Formation is dominated by lithic-rich breccia, coherent intrusions, hyaloclastite, coherent lava, vitric tuffaceous sandstone–siltstone and subordinate pumice breccia-sandstone, all of rhyolite-4, transitional-1 composition, and weakly to moderately feldspar-porphyritic and only minor quartz phenocrysts. The local occurrence of samples characterized as rhyolite-1 within the Ski Hill Formation are of calc-alkaline-1 affinity and are interpreted as intrusions that are time-equivalent and co-magmatic with the overlying Buchans River Formation.

Buchans River Formation

The Buchans River Formation is characterized by hyaloclastite, coherent lava, intrusions and pumiceous volcaniclastic facies of rhyolite-1, calc-alkaline-1 composition (upper Buchans River Formation throughout the camp, and lower Buchans River Formation at Clementine) and rhyolite 4 of intermediate transitional-1-calc-alkaline-1 affinity (lower Buchans River Formation at Oriental-Sandfill–Rothermere; Figure 5A, B). Rhyolite-4 facies are also common in the underlying Intermediate Footwall member. However, rhyolite-4 facies within the Buchans River Formation are intermediate between transitional-1 and calc-alkaline-1 (Th/Yb > 2.5), whereas in the Intermediate Footwall member they are of transitional-1 affinity (Th/Yb < 2.5). Volcanic facies of the upper Buchans River Formation (Buchans Camp member) are distinctly quartz and feldspar porphyritic throughout the area, whereas the lower Buchans River Formation contains both strongly and weakly to moderately porphyritic rocks, including rock units with abundant quartz phenocrysts (Oriental-Sandfill member) and units with minor to moderate abundance of quartz phenocrysts (Clementine member).

Sandy Lake Formation

Rocks of the Sandy Lake Formation are characterized by abundant basalt-2 of transitional-1 affinity and rhyolite-1 and 4 of calc-alkaline-1 affinity (Figure 5A, B). Basalt-2 includes pillow lava, fire fountain breccia and transported volcaniclastic facies. The rhyolitic rocks include intrusions and abundant moderate to well sorted, quartz–feldspar crystal-lithic volcanic breccia-sandstone–siltstone that is interpreted as reworked detritus from terrestrial pyroclastic eruptions at the basin margin or an emergent horst block within the basin. Rocks within the Sandy Lake Formation can be distinguished from the Ski Hill Formation by the abundance of well-sorted, crystal-rich sandstone (arkose).

SWIR ALTERATION STUDIES

The following discussion provides a summary of the results obtained from the examination of select drillholes using short wavelength infrared (SWIR) spectrometry to characterize the mineralogy of hydrothermal alteration that was historically described as "sericite" alteration. SWIR spectrometry provides the ability to obtain mineralogical information on the crystallinity and/or compositional variations associated with certain mineral groups, such as white micas (*e.g.*, paragonite, muscovite and phengite). Illite variants of these white mica minerals are expressed by the spectral software (The Spectral Geologist; TSG™) as either paragonitic-illite, muscovitic-illite, or phengitic-illite (*see* below). The variation in the Al-OH absorption feature (~2200 nm) is one example of a calculated scalar from the spectral data that can be utilized to gain insight regarding the compositional differences within various white mica minerals (*e.g.*, paragonite (2180–2195 nm), muscovite (2195–

2215 nm) and phengite (2215–2225 nm); Pontual *et al.*, 1997; AusSpec, 2008). The position of the Al-OH feature also can be used as a hydrothermal pH indicator, with shorter wavelengths representative of more acidic hydrothermal conditions (Halley *et al.*, 2015). Spectral measurements were collected using either a TerraSpec® Pro or TerraSpec® Halo spectrometer, and these spectra were subsequently processed using The Spectral Geologist (TSG™) software (version 8.0.7.4) to obtain mineral identifications. This software provides the two most abundant minerals present (Min 1 and Min 2) for individual spectral analysis by comparing each spectra to a reference library of known minerals.

Previous studies that have investigated the alteration associated with mineralization in the Buchans area, include work by Henley and Thornley (1981), Thurlow (1981), Winter (2000) and van Hees (2011). For the current study, select drillholes from the Buchans area were examined to determine the spectral signature of the hydrothermal alteration developed in the immediate footwall to *in situ* massive sulphide mineralization at the Lucky Strike deposit (Figure 1). In addition, drillholes from the Rothermere deposit were examined to compare the spectral signature of the alteration associated with transported ore proximal (<1 km) to *in situ* mineralization (Lucky Strike deposit) with that of transported ore from the Sandfill prospect, which is also interpreted to be proximal to a hydrothermal vent (Allen and Schofield, 2023), but displays a distinctly different alteration signature. Finally, the Powerhouse prospect (Figure 1) is discussed due to its association with a strong zone of hydrothermal alteration hosted within a thick sequence of felsic volcanic rocks, presumed to be correlative with the Buchans River Formation (Saunders *et al.*, 1996, 1998; Harris *et al.*, 1999; Saunders *et al.*, 2000), indicating a potential footwall environment to VMS mineralization.

LUCKY STRIKE

Spectral data collected in the area of the Lucky Strike deposit are representative of footwall alteration developed immediately beneath *in situ* massive sulphide mineralization. Here, extensive footwall alteration persists up to 130 m below the mineralized horizon. Within the footwall zone of the Lucky Strike deposit, the alteration developed immediately beneath the massive sulphide mineralization is dominated by muscovitic illite, siderite, montmorillonite and lesser chlorite. In drillhole H-08-3356 (Plate 11), the upper drillhole consists of massive sulphide mineralization crosscut by abundant carbonate veining. The SWIR spectral data from this mineralized zone is dominated by aspectral (no identifiable mineral signature) and siderite, along with lesser muscovite, muscovitic illite, chlorite and montmorillonite developed toward the base of the zone (Figure 6). Upon transitioning into the underlying footwall, muscovitic illite and lesser chlorite become the dominate alteration minerals. Within these footwall rocks, there is a general trend from approximately 200 m depth toward the base of the massive sulphide mineralization (~50 m depth) that illustrates a shift in the Al-OH spectral feature to shorter spectral wavelengths (from ~2210 to 2202 nm) with decreasing distance from mineralization (Figure 6).

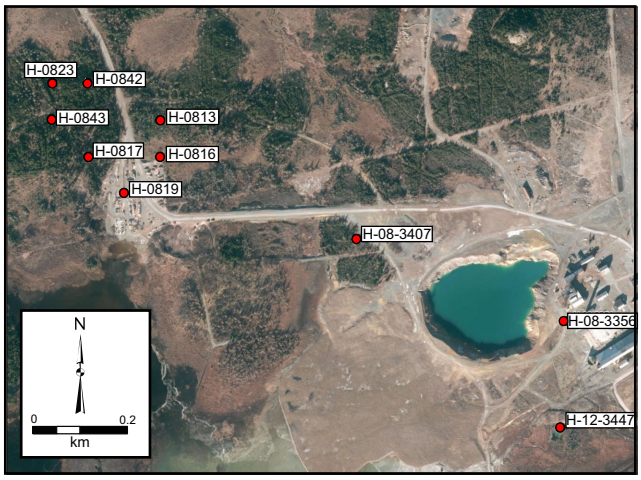

Plate 11. *Aerial image of the Lucky Strike and Rothermere deposits outlining the geographical distribution of select diamond drillholes.*

In drillhole H-08-3407 (Plate 11), the examined interval (130–165 m) targeted footwall rocks hosting stockwork mineralization of the Lundberg deposit (Plate 12). Here, the "sericite" alteration, locally characteristically bright green, overprints basaltic rocks of the Ski Hill Formation and is classified as a mixture of muscovitic illite–montmorillonite based on spectral data. The SWIR data from this select interval displays consistent Al-OH values (~2207 nm) throughout. These values are similar to those obtained from the rocks immediately underlying massive sulphide mineralization in drillhole H-08-3356, but given the narrow interval that was investigated, no systematic variation of the Al-OH feature was observed.

ROTHERMERE

The Rothermere deposit represents an example of transported ore, located proximal (<1 km) to *in situ* massive sulphide mineralization, for which select intervals of both mineralized and barren drillholes were examined. In drillhole H-0817 (Plate 11), two intervals (100–260 m; 260–470 m) were examined containing distinct structural panels hosting similar volcanic facies, but only one panel contains hydrothermal alteration and related mineralization (based on

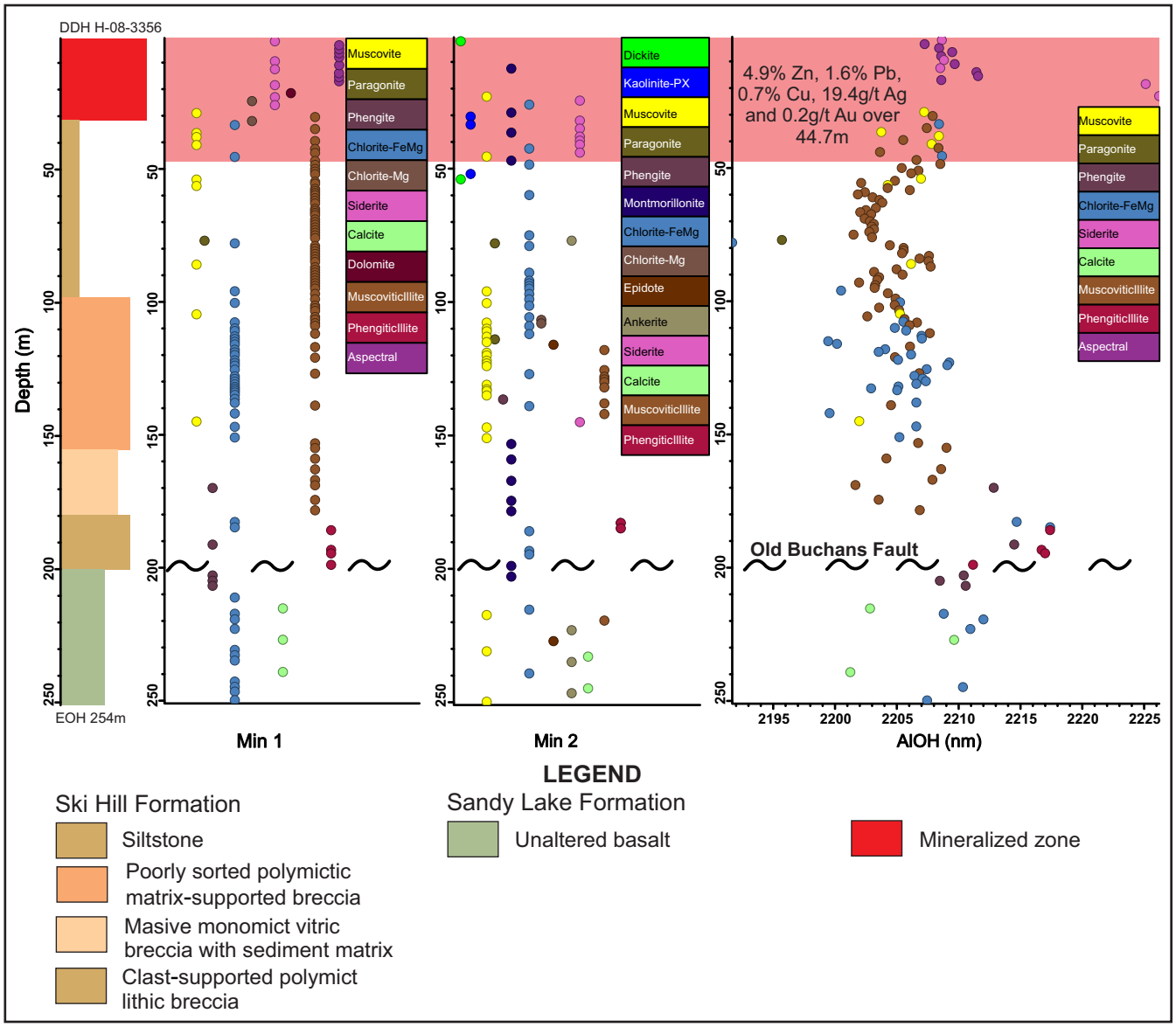

Figure 6. *Strip log for DDH H-08-3356, outlining the distribution of massive sulphide mineralization and underlying units, along with corresponding spectral data showing the distribution of mineral 1 (Min 1), mineral 2 (Min 2) and the related Al-OH absorption wavelength; Lucky Strike deposit. Assay values taken from Moore* et al. *(2009). For the location of the drill-hole, refer to Plate 11.*

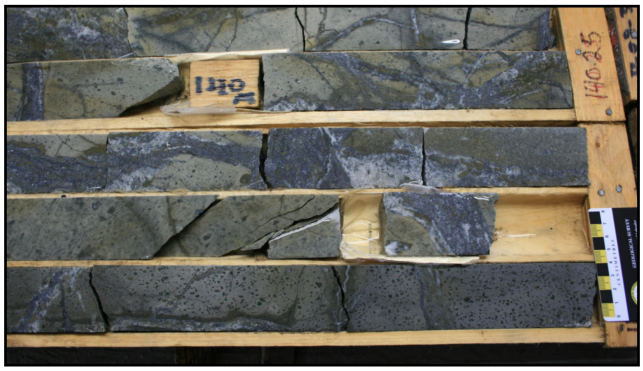

Plate 12. *Stockwork polymetallic sulphides and carbonate veining hosted within basaltic rocks of the Ski Hill Formation, associated with intense muscovitic illite alteration; DDH H-08-3407 140 m, Lundberg deposit.*

industry logging). The first structural panel (100–260 m) is characterized by phengite and phengitic illite white mica alteration of the rhyolite hyaloclastite unit, displaying Al-OH wavelengths between 2015–2025 nm (Figure 7). This unit displays weak to moderate white mica alteration of the feldspar phenocrysts and supporting matrix (Plate 13A).

Within the second structural panel, the upper portion of a rhyolite hyaloclastite unit (260–430 m), overlying the mineralized zone, displays similar alteration signatures to that of the overlying structural panel, and is dominated by phengite and phengitic illite alteration, with Al-OH wavelengths between 2015–2025 nm (Plate 13B; Figure 7). However, in the area of the mineralized zone there is an abrupt shift in the Al-OH wavelength values to shorter spectral wavelengths (~2200 nm) in association with the development of muscovitic illite and lesser muscovite and montmorillonite alteration (427–455 m; Plate 13C; Figure 7). The sharp shift to phengite dominated alteration immediately above the mineralized zone may indicate a struc-

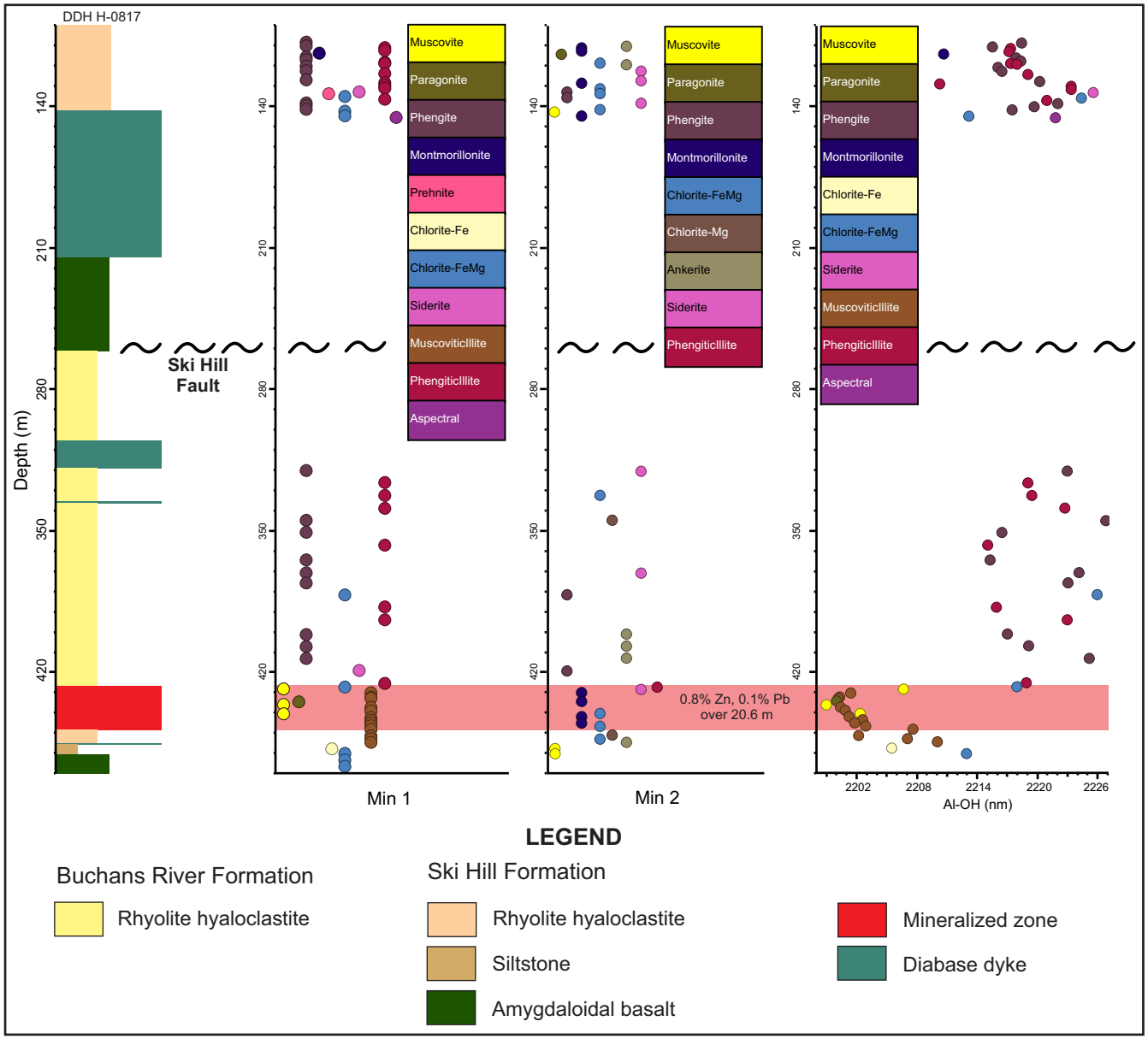

Figure 7. *Partial strip log for DDH H-0817, outlining the distribution of the mineralized horizon and significant fault structures. Also shown is the corresponding spectral data, outlining the distribution of mineral 1 (Min 1), mineral 2 (Min 2) and the related Al-OH absorption wavelength; Rothermere deposit. Assay values taken from historical ASARCO drill logs. For the location of the drillhole, refer to Plate 11.*

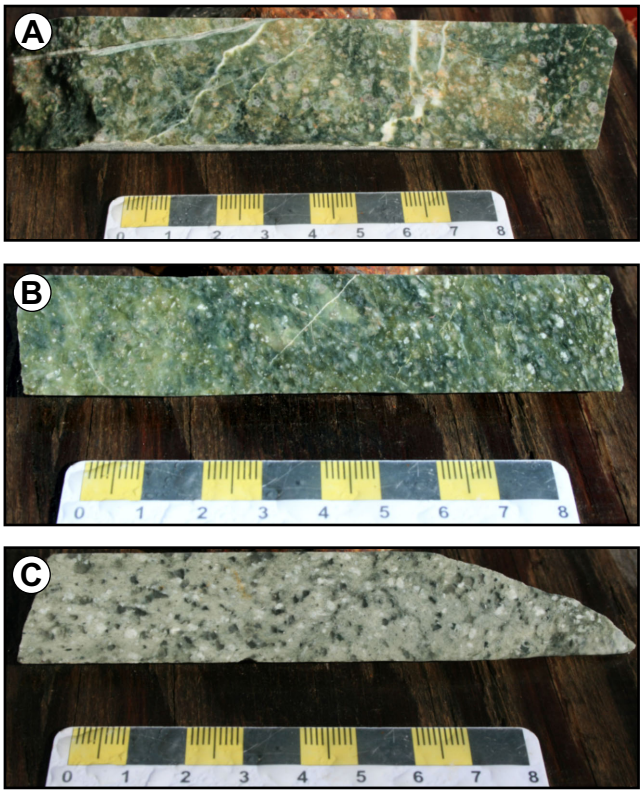

Plate 13. *Representative photographs of alteration from the area of the Rothermere deposit. A) Rhyolite of the Buchans River Formation, containing phengite alteration; DDH H-813 130 m; B) Similar unit to that shown in (A), containing phengitic illite alteration; DDH H-813 220 m; C) Strongly altered rhyolite, Buchans River Formation, containing paragonite–montmorillonite alteration; DDH H-813 380 m. For the location of the drillhole, refer to Plate 11.*

turally modified contact, as spectral data from other drillholes in this area locally display a more gradational transition of the Al-OH feature to longer wavelengths over approximately 30 m (*see* below).

Drillhole H-0819 is located on the margin of the mineralized zone within the Rothermere deposit (Plate 11), and only intersected weakly developed mineralization over approximately 3 m (Figure 8). Despite the weakly developed mineralization, this drillhole still displays the distinct shift of the Al-OH wavelength feature to shorter spectral wavelengths (~2202 nm) in association with the mineralized horizon. In this drillhole, the hangingwall rocks also appear to display the effects of hydrothermal alteration related to the mineralized horizon, marked by a gradational transitioning up-section to longer wavelength Al-OH values (~2225 nm), over approximately 30 m (Figure 8). Allen and Schofield (2023) also noted weak alteration of the hangingwall rocks in this area, which may indicate these rocks were deposited while hydrothermal fluids related to the VMS system remained active, and thus affected the basal portion of this unit.

SANDFILL

The area of the Sandfill prospect (Figure 2) targeted a second example of transported ore clasts, but one that occurred without significant visible hydrothermal alteration within the host breccia–conglomerate. SWIR investigations of drillcore from the area display some key differences when compared with the spectral signature of transported ore from the Rothermere deposit.

Spectral data from drillhole H-1683 illustrates that the hangingwall rocks of the Airport Thrust fault display Fe- and Fe–Mg-chlorite, along with lesser muscovite, paragonite, muscovitic illite and paragonitic illite alteration (Figure 9). The hangingwall sequence is dominated by the Woodmans Brook volcanic rocks of Thurlow (2001), which have been correlated with the Lundberg Hill Formation by Allen and Schofield (2023). Local zones of mica-dominated alteration are commonly centred on felsic dykes (*e.g.*, ~120 m, Figure 9). Likewise, a distinct "prominent quartz" unit within the hangingwall sequence (155–170 m; 190–260 m) is characterized by muscovitic illite-, paragonitic illite- and paragonite-dominated spectral signatures. The alteration associated with this unit is interpreted as a syn-depositional hydrothermal alteration related to the formation of the pyroclastic unit, which is locally noted by Allen and Schofield (2023) to display welded textures. This interpretation is supported because this alteration does not affect the underlying rocks (Plate 14), and is therefore not related to hydrothermal alteration associated with VMS mineralization as seen elsewhere in the region. Similarly, the general decrease in the Al-OH wavelength feature observed with increasing depth (80 to 250 m, Figure 9), is not attributed to hydrothermal alteration associated with the development of VMS mineralization, but is instead related to the deposition of the distinct "prominent quartz" unit mentioned above. A sharp contrast in the Al-OH wavelength feature is observed across the Airport Thrust fault, transitioning from shorter wavelength white mica minerals in the hangingwall (<2200 nm) to longer wavelength (>2212 nm), phengite-dominated, white mica minerals within the footwall. The footwall rocks are dominated by arkosic sandstone of the Sandy Lake Formation, which overlie polymict lithic breccia–conglomerate of the Buchans River Formation, that hosts rare ore clasts. The spectral signature of this ore horizon is indistinguishable from that of the overlying post-alteration Sandy Lake Formation (Figure 9), indicating no significant hydrothermal alteration is associated with the deposition of this unit.

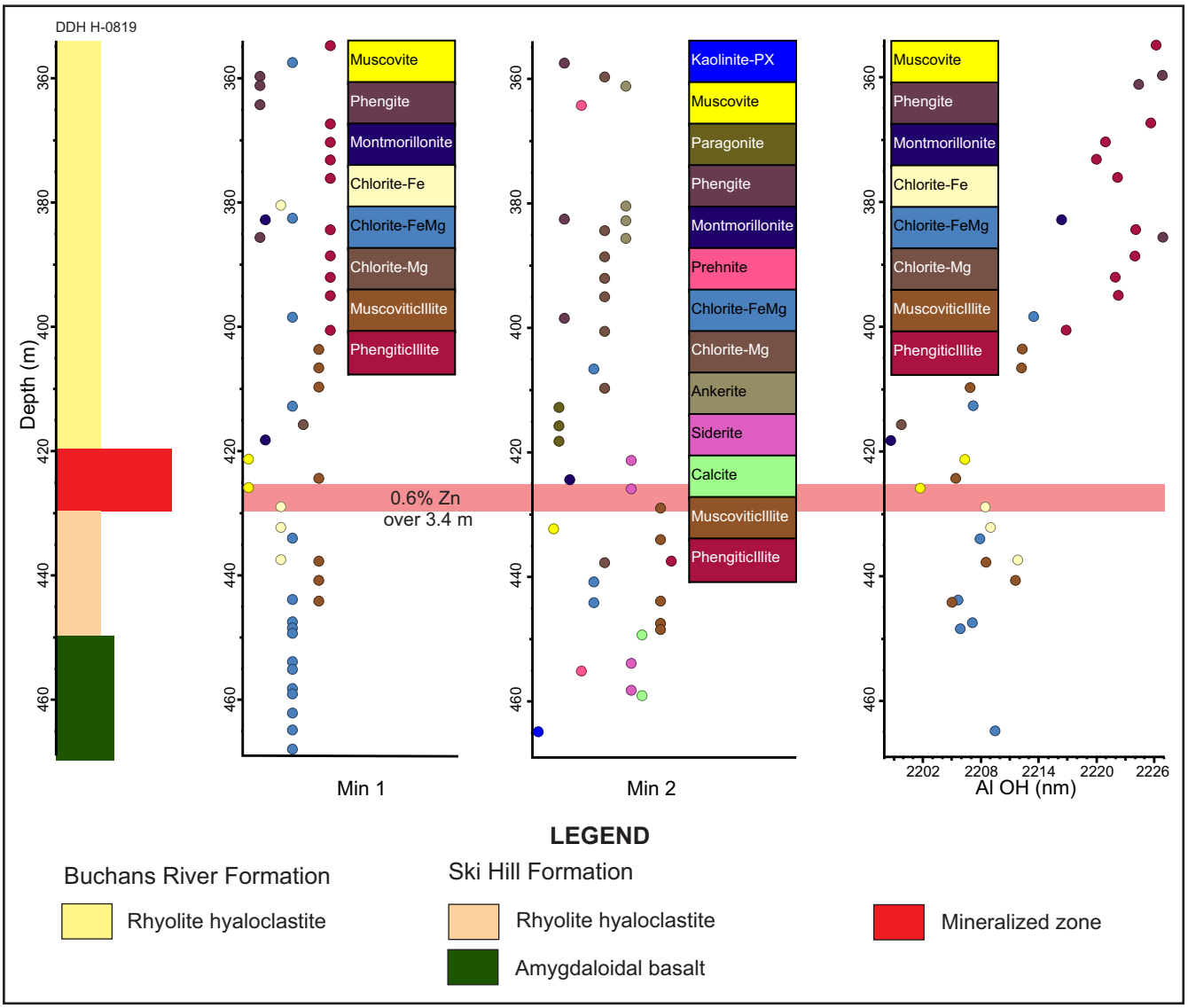

Figure 8. *Partial strip log for DDH H-0819, outlining the distribution of the mineralized horizon and the corresponding spectral data showing the distribution of mineral 1 (Min 1), mineral 2 (Min 2) and the related Al-OH absorption wavelength; Rothermere deposit. Assay values taken from historical ASARCO drill logs. Note the mineralized horizon in this drillhole is approximately 60 m from ore grade mineralization. For the location of the drillhole, refer to Plate 11.*

POWERHOUSE

The area of the Powerhouse prospect displays a similar structural setting to that of the Sandfill prospect, but is dominated by felsic volcanic rocks of the Buchans River Formation within the footwall of the Airport Thrust fault (Figure 2). This area is not associated with any known massive sulphide or transported ore, but rather represents a zone of intense hydrothermal alteration that remains open and untested to the east and northeast (Saunders *et al.*, 2000).

In this area, the hangingwall rocks of the Airport Thrust fault predominantly display Fe- and Fe–Mg-chlorite, along with lesser muscovite, paragonite, and paragonitic illite (Figure 10). Below the thrust fault, footwall rocks display variable white mica alteration and intermittent base- and precious-metal enrichment. Spectral data from the Powerhouse area supports an overall north–northeastward increase in the intensity of white mica alteration, up to the current limits of diamond drilling. This altered sequence is subsequently truncated at depth by the Buchans River–Old Buchans thrust fault, below which there is a marked shift to phengite and Fe–Mg-chlorite dominated spectral signatures associated with sandstone and interbedded conglomerate and mafic volcanic rocks of the Sandy Lake Formation, respectively (Figure 10).

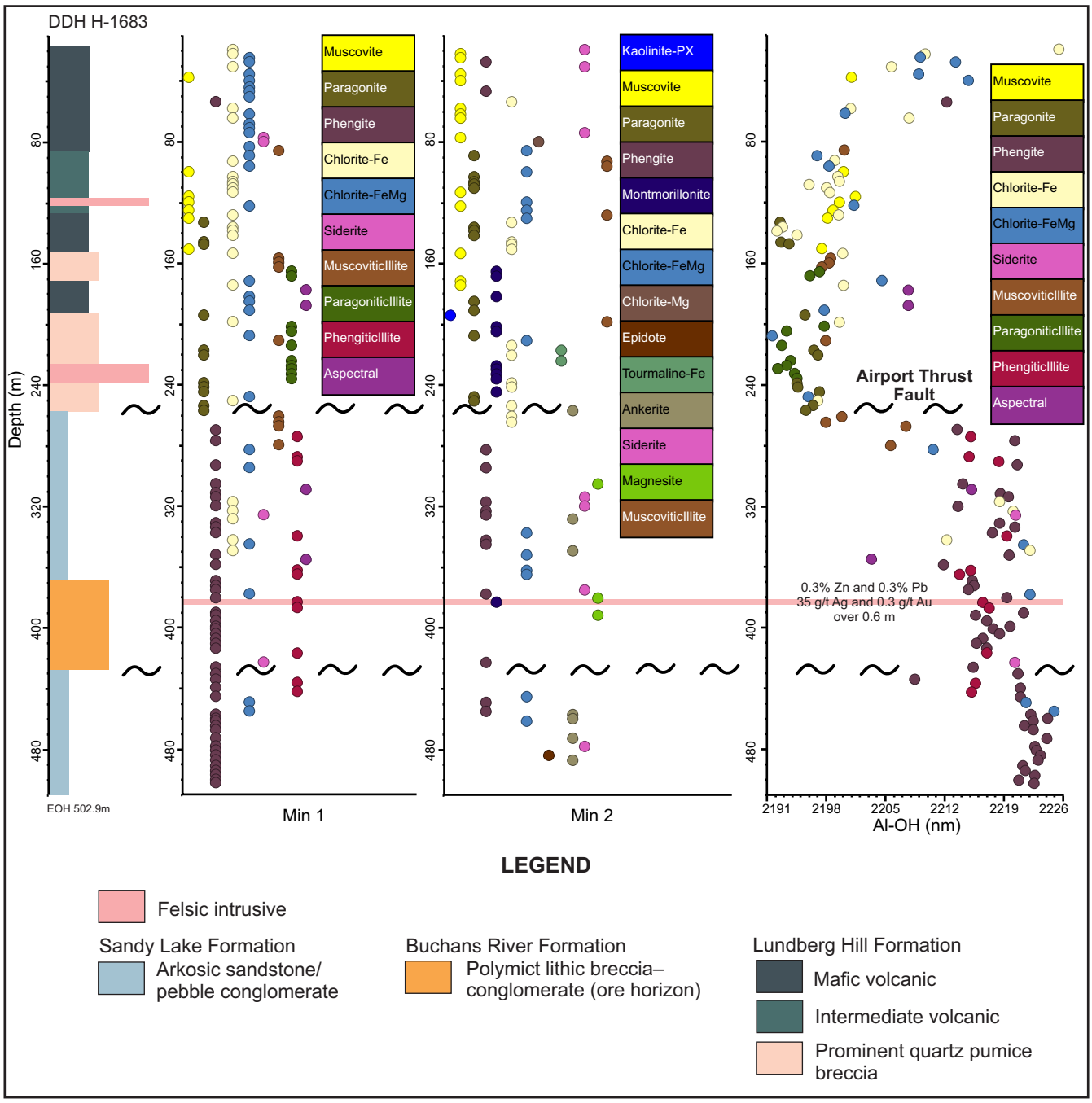

Figure 9. *Strip log for DDH H-1683, outlining the distribution of the spectral data, mineral 1 (Min 1) and mineral 2 (Min 2), along with the related Al-OH absorption wavelength and the location of select mineralization; Sandfill prospect. Assay values taken from Harris* et al. *(1997). For the location of the drillhole, refer to Figure 2.*

The northeastern most drillhole from this prospect displays the strongest alteration observed within the area. This drillhole, DDH BE-97-020, collars directly into altered felsic volcanic rocks of the Buchans River Formation, with the first 180 m consisting of paragonitic illite–montmorillonite-dominated alteration (Figure 11). This interval also contains localized zones of base- and precious-metal enrichment. For example, paragonitic illite–montmorillonite-dominated alteration, associated with a pyritic stringer zone, assayed 0.1 g/t Au and 3.1 g/t Ag over 4.4 m (Plate 15A; Saunders *et al.*, 1998, 2000). The same alteration is also locally host to disseminated sulphide mineralization assaying 0.7% Zn and 0.2% Pb over 8.5 m (Plate 15B; Saunders *et al.*, 1998). Below the paragonitic illite–montmorillonite-dominated

Plate 14. *Prominent quartz welded massive monomict vitric (± lithic) breccia without jigsaw-fit (2D), characterized by muscovitic illite and paragonitic illite spectral signatures, interbedded with relatively unaltered mafic volcanic rocks characterized by Fe–Mg-chlorite; DDH H-1683 156–180 m.*

alteration, Al-OH values display a moderate increase to longer spectral wavelengths (~2199 nm), transitioning into muscovite–muscovitic-illite-dominated alteration at depth. The white mica alteration persists to the Buchans River–Old Buchans thrust fault (~350 m) where it is structurally truncated (Figure 11). Below the thrust fault, there is a prominent shift in the overall Al-OH values to longer wavelengths, characteristic of the phengite spectral signature associated with the siliciclastic rocks of the Sandy Lake Formation (Figure 11).

DISCUSSION

Contrary to previous studies, detailed re-logging of drillcore from the Buchans area has demonstrated that most facies developed within the local Buchans stratigraphy are considered to be related to lava flows, lava domes and shallow-level subvolcanic intrusions (sills). Pyroclastic rocks (true tuffs) are subordinate; the pyroclastic facies that are present appear to be related to the emplacement and evolution of the lavas. Some rock units are very difficult to distinguish by mapping or core logging alone and some others are difficult to distinguish by geochemistry. However, a combination of (a) volcanic facies characteristics including the amount and type of phenocrysts, (b) the volcanic composition from Zr/Al_2O_3 and Al_2O_3/TiO_2 ratios, and (c) magmatic affinity from especially the Th/Yb ratio, enables all rhyolitic units to be distinguished from each other.

The ore-bearing stratigraphic interval of the Buchans area is interpreted to comprise a series of four submarine rhyolite lava dome–cryptodome eruption packages (volcanoes), rather than a caldera filled with pyroclastic debris as was interpreted by some previous workers (*e.g.*, Kirkham and Thurlow, 1987). The rhyolite dome–cryptodome volcanoes are similar to Miocene submarine rhyolite volcanoes that host the Kuroko VMS deposits in Japan (*cf.* Horikoshi, 1969). The massive sulphide ores and ore-clast breccia units at Buchans formed in response to hydrothermal, volcanic and tectonic events during the emplacement of these rhyolite dome–cryptodome volcanoes. Of the eleven volcanic geochemical subdivisions, the Intermediate Footwall member and the Oriental-Sandfill member are characterized by rhyolite-4 composition, whereas the Clementine member and Buchans Camp member are characterized by rhyolite-1 composition. Ore horizons occur at the top of the Intermediate Footwall member, at the top of the Oriental-Sandfill member, within and at the top of the Clementine member, and within the basal part of the Buchans Camp member. Consequently, felsic volcanic facies of both rhyolite-1 and rhyolite-4 composition can occur below and above an ore horizon and thus volcanic composition alone does not discriminate between footwall and hangingwall. Furthermore, both rhyolite-1 and rhyolite-4 subdivisions include feldspar-phyric units with only rare or minor (<4%) quartz phenocrysts as well as units with abundant (4–10%) quartz phenocrysts. Although the upper part of the Buchans River Formation can be readily distinguished from the Intermediate Footwall member (rhyolite-1, and -4, respectively) in the type area around Lucky Strike–Oriental-Sandfill, the rocks in between, and all felsic rocks below the upper part of the Buchans River Formation at the Clementine deposit, are difficult to discriminate as to whether they should be mapped as Intermediate Footwall member or Buchans River Formation. However, by experimenting further with comparison of stratigraphic position and immobile element ratios, it was found that complementing the facies characteristics and ratios between Zr, TiO_2 and Al_2O_3 with a measure of magmatic affinity, in particular the Th/Yb ratio, enables all the various felsic volcanic packages to be distinguished.

The four rhyolite dome–cryptodome eruption packages (volcanoes) and their distinguishing physical and chemical characteristics comprise, in stratigraphic order, from top to bottom:

- Buchans Camp member; forms the entire upper Buchans River Formation. Composition: strongly quartz–feldspar-phyric rhyolite-1 of calc-alkaline-1 affinity.

- Clementine member of the lower Buchans River Formation in the Clementine area. Composition: moderately feldspar-minor quartz-phyric rhyolite-1 and dacite of calc-alkaline-1 affinity.

- Oriental-Sandfill member of the lower Buchans River Formation in the Old Buchans–Oriental-Sandfill area.

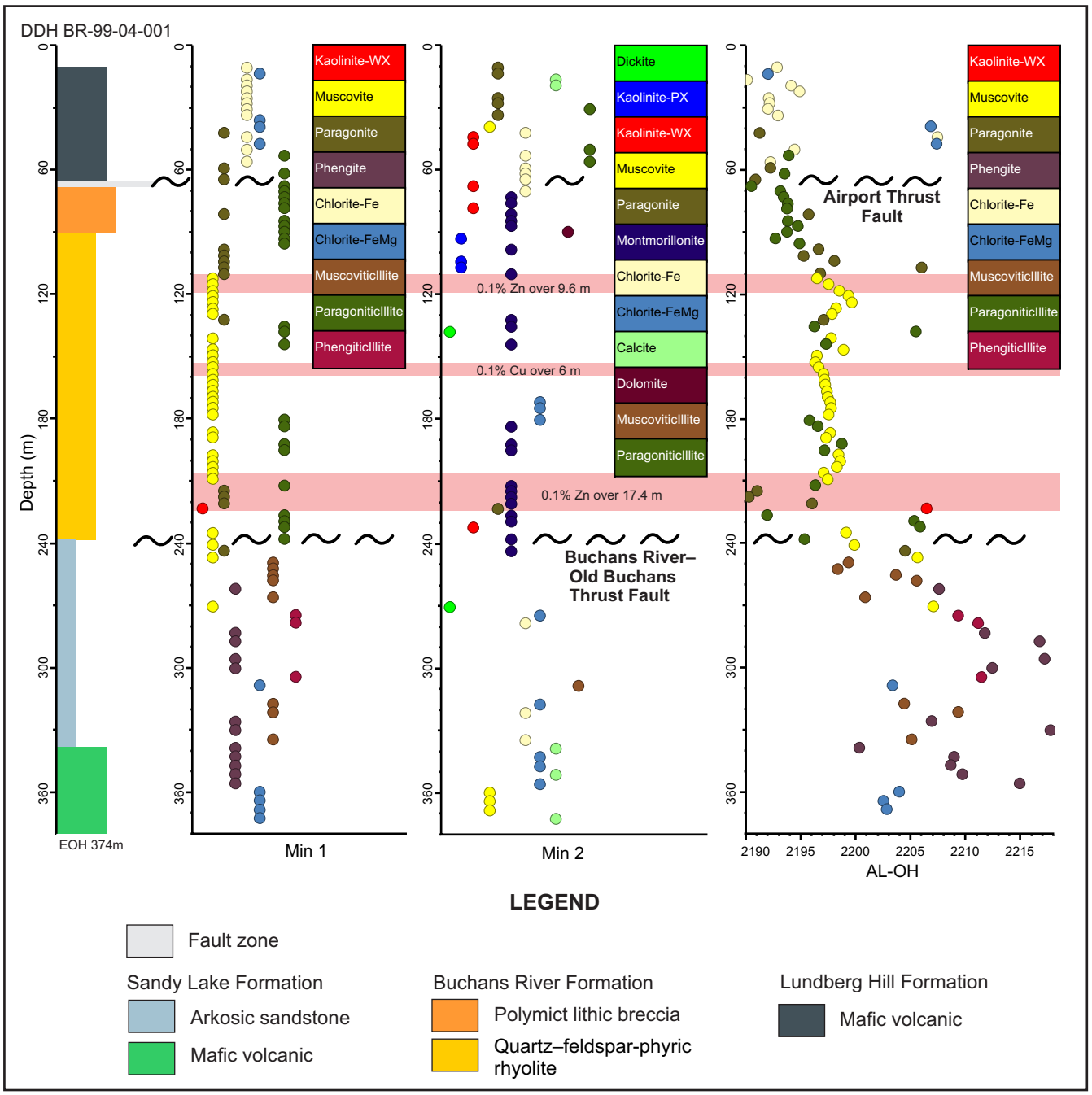

Figure 10. *Strip log for DDH BR-99-04-001, outlining the distribution of the spectral data, mineral 1 (Min 1) and mineral 2 (Min 2), along with the related Al-OH absorption wavelength and the location of select mineralization; western portion of the Powerhouse prospect. Assay values taken from Harris* et al. *(1999). For the location of the drillhole, refer to Figure 2.*

Composition: strongly quartz–feldspar-phyric rhyolite-4 of intermediate transitional-1 - calc-alkaline-1 affinity.

- Intermediate Footwall member of the Ski Hill Formation in the Lucky Strike–Old Buchans North-Oriental-Sandfill areas. Composition: moderately feldspar-rare quartz-phyric, rhyolite 4 of transitional 1 affinity.

Following widespread felsic and mafic volcanism of the Lundberg Hill Formation, in a mixed subaerial and submarine environment, and subsequent submarine mafic volcan-

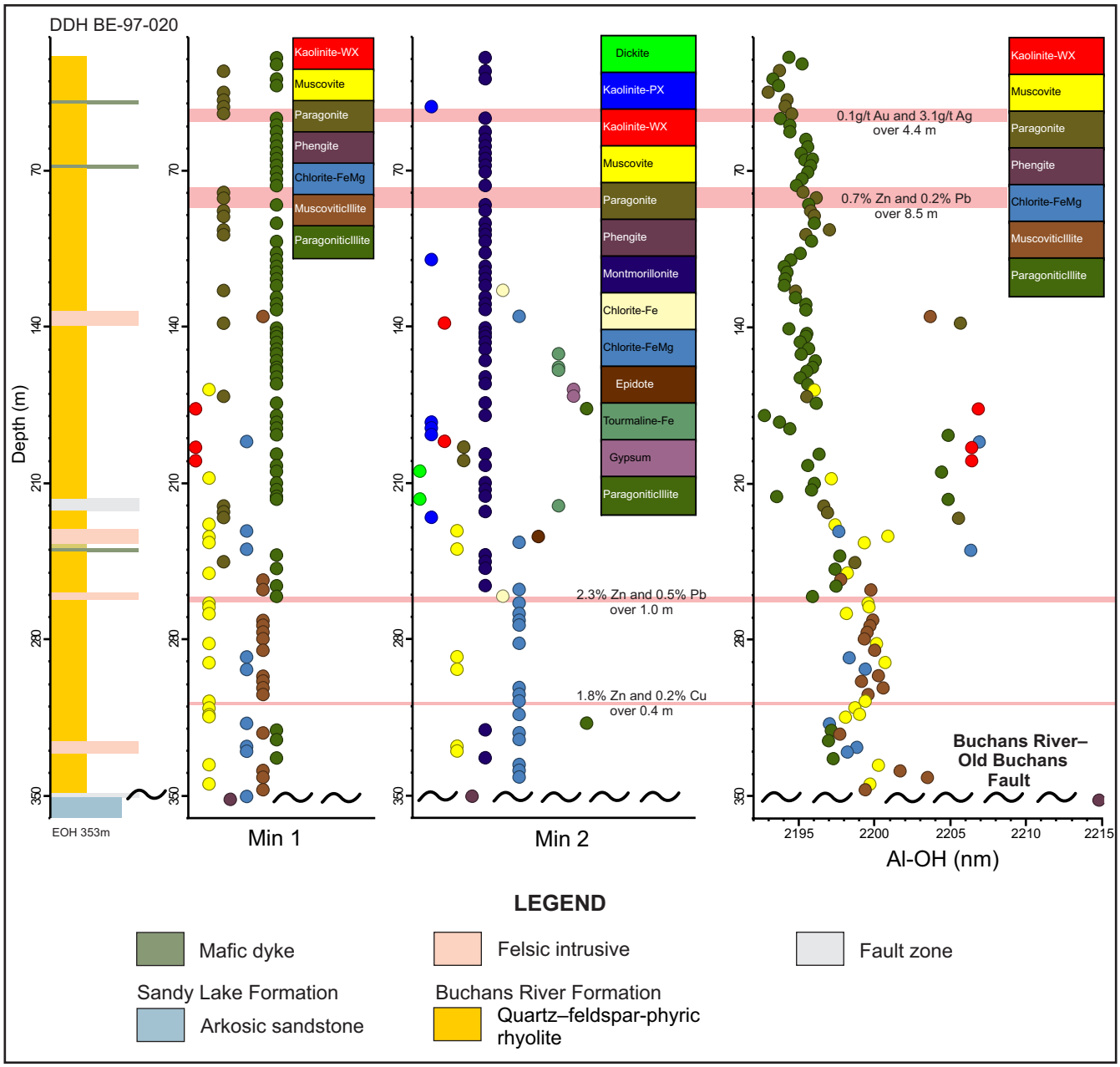

Figure 11. *Strip log for DDH BE-97-020, outlining the distribution of the spectral data, mineral 1 (Min 1) and mineral 2 (Min 2), along with the related Al-OH absorption wavelength and the location of select mineralization; eastern portion of the Powerhouse prospect. Assay values taken from Saunders* et al. *(1998, 2000). For the location of the drillhole, refer to Figure 2.*

ism of the Ski Hill Formation, the ore-host succession of submarine rhyolite dome volcanoes formed. Vents for the rhyolite domes and associated pyroclastic facies likely occurred along or adjacent to synvolcanic faults. Hydrothermal eruptions accompanied and followed dome emplacement and the first massive sulphide deposits formed from effusion of these hydrothermal solutions. Vents for the hydrothermal eruptions and sulphide mineralization were within the rhyolite domes, most likely close to the volcanic dome vents and also along synvolcanic faults. Formation of massive sulphide ceased after the initial eruptions of the fourth rhyolite dome–cryptodome package. The stratigraphic order of the dome volcanoes corresponds to a progression in magmatic affinity from transitional, to intermediate transitional calc-alkaline to strongly calc-alkaline. This is unlikely to be coincidence and appears to document a magmatic evolution of Buchans felsic volcanism at the time of VMS mineralization.

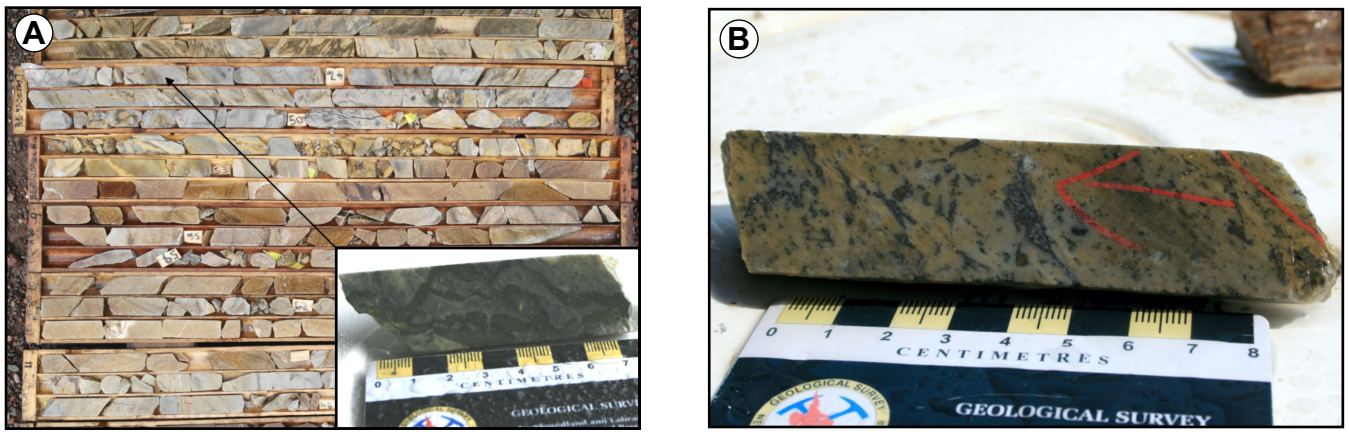

Plate 15. *A) Paragonitic illite–montmorillonite alteration crosscut by pyrite-rich stringer mineralization hosting anomalous Zn and Pb, along with Au, Ag, As and Hg enrichment, and localized zones of hydrothermal brecciation; DDH BE-97-020 43–68 m, Powerhouse prospect; B) Quartz–feldspar-phyric rhyolite, displaying paragonitic illite–montmorillonite alteration and hosting disseminated sulphide mineralization. Sample contains 1.4% Zn, 0.15% Pb, 1.3 g/t Ag, 2.4 ppm Hg and 51 ppb Au over 0.7 m; DDH BE-97-020 81 m.*

The use of SWIR to evaluate the spectral signature of hydrothermal alteration developed proximal to *in situ* massive sulphide mineralization demonstrates that footwall rocks are dominated by shorter wavelength white mica alteration minerals (*e.g.*, muscovite, muscovitic illite) and lesser montmorillonite. The development of this alteration is best illustrated by the Al-OH spectral wavelength feature, which can be numerically modelled in downhole plots. Where stratigraphic sequences remain intact, a systematic shift toward shorter spectral wavelengths is observed with decreasing distance from mineralization, locally both within the footwall and hangingwall rocks. However, caution must be used in the interpretation of this spectral data, as similar alteration signatures (*e.g.*, paragonitic illite–montmorillonite) are also locally associated with distinct geological units (*e.g.*, prominent quartz pumice breccia, DDH H-1683), which are not attributed to hydrothermal alteration associated with a vent proximal environment.

Distal from mineralized zones, rocks that are compositionally similar to those immediately adjacent to mineralization are characterized by longer wavelength white mica minerals (*e.g.*, phengite, phengitic illite). Similar features are developed in association with the transported ores, whereby transported ores deposited proximal to the source hydrothermal vent (*e.g.*, Rothermere deposit), display a shift in the Al-OH feature toward shorter spectral wavelengths in association with the mineralized horizon. However, transported ores that are distal from any known *in situ* massive sulphide (*e.g.*, Sandfill prospect) display a distinctly different spectral signature; one that is characterized by longer spectral wavelengths, which is characteristic of less altered country rock, and is supportive of a distal depositional environment relative to mineralizing hydrothermal vents.

The identification of intensely altered felsic volcanic rocks hosting argillic alteration within the footwall of the Airport thrust fault in the area of the Powerhouse prospect, which is >1.0 km from any known massive sulphide mineralization, highlights the area as a prospective mineralizing environment. Here, thick intervals of paragonitic illite–montmorillonite white mica alteration locally dominate the host felsic volcanic rocks, along with associated hydrothermal brecciation and stockwork-style mineralization. Similar footwall alteration signatures have been noted elsewhere, both within the Buchans–Roberts Arm and Tulks Volcanic belts, proximal to VMS mineralization (*cf.* Sparkes and Hinchey, 2023). The Powerhouse alteration zone, when combined with the recently identified advanced argillic alteration in the area of the Tower prospect some 7-km along strike to the east (Sparkes, 2022), highlights a zone of strong hydrothermal alteration developed within a poorly understood and underexplored portion of the Buchans camp, which, based on the spectral data, is prospective for VMS mineralization.

CONCLUSION

Detailed facies mapping, used in combination with geochemical analysis, provides an effective means of reconstructing the volcanic stratigraphy of the Buchans area, allowing for the delineation of prospective ore horizons. Results from the detailed graphic logging of drillcore provides insight into the depositional environment of the Buchans River Formation, and related VMS mineralization, which can be subdivided into two camp-wide and up to three more localized ore horizons. This mineralization is associated with the emplacement of four rhyolite dome–cryptodome eruption packages, with the youngest represented by the

Buchans camp member, the deposition of which marks the cessation of hydrothermal activity within the area.

SWIR investigations of the hydrothermal alteration associated with mineralization illustrates key characteristics of the footwall environment that are analogous with the development of VMS mineralization elsewhere in the region. Detailed downhole collection of spectral data can aid in the recognition of potential ore horizons, in addition to highlighting prospective environments that have yet to be fully evaluated (*e.g.*, Powerhouse–Tower trend). These novel techniques can be applied elsewhere in the region and may aid future exploration in delineating new prospective environments for massive sulphide mineralization.

ACKNOWLEDGMENTS

Buchans Minerals Corporation personnel are thanked for allowing the publication of elements of this report and for providing insight during some of these investigations. The authors extend appreciation to Paul Moore and David Butler, in particular, for providing critical local knowledge and helpful discussions. William Oldford and Derrick Keats are gratefully acknowledged for assistance in the Buchans core library.

REFERENCES

Allen, R.L.
1992: Reconstruction of the tectonic, volcanic and sedimentary setting of strongly deformed Cu-Zn massive sulfide deposits at Benambra, Victoria. Economic Geology, Volume 87, pages 825-854.

Allen, R. and Schofield, M.
2023: Volcanic facies, lithogeochemistry and vectors to ore at Buchans massive sulphide camp, Newfoundland. Stage 1 Final Report. Unpublished internal company report prepared for Buchans Minerals Resources.

AusSpec International Ltd.
2008: Spectral analysis guides for mineral exploration (GMEX): Practical applications handbook. 3rd edition.

Barrett, T.J.
2012: Lithogeochemistry and chemostratigraphy of volcanic rocks at Buchans, Newfoundland. Newfoundland and Labrador Geological Survey, Assessment File 12A/15/1710, 1854 pages.

Cole, J.W.
1970: Structure and eruptive history of the Tarawera Volcanic Complex. New Zealand Journal of Geology and Geophysics, Volume 13, pages 879-902.

Halley, S.W., Dilles, J.H. and Tosdal, R.M.
2015: Footprints: Hydrothermal alteration and geochemical dispersion around porphyry copper deposits. SEG Newsletter, Issue Number 100, pages 11-17.

Harris, J., Saunders, P. and Reed, L.E.
1999: First year, third year supplementary, fourth year supplementary and seventh year supplementary assessment report on diamond drilling exploration and relogging of diamond drillcore for licence 4272 on claim blocks 7916-7917 and 7919-7921 and claims 16512-16514, licence 4294 on claim block 7896, licence 4805 on claim 16398, licence 4806 on claims 16397, 16399-16401, 16424-16426 and 17686-17688, licence 4823 on claims 16431-16432 and licences 4974M and 6973M on claims in the Buchans area, central Newfoundland. Newfoundland and Labrador Geological Survey, Assessment File 12A/15/0946, 304 pages.

Harris, J., Saunders, P. and Wilton, D.H.C
1997: First year supplementary and fourth year assessment report on relogging of diamond drillcore for licence 4317 on claim block 7984 and licence 4806 on claims 16397, 16399-16401, 16424-16426 and 17686-17688 in the Buchans area, central Newfoundland. Newfoundland and Labrador Geological Survey, Assessment File 12A/15/0877, 169 pages.

Henley, R.W. and Thornley, P.
1981: Low grade metamorphism and the geothermal environment of massive sulphide formation, Buchans, Newfoundland. *In* The Buchans Orebodies: Fifty Years of Mining and Exploration. *Edited by* E.A. Swanson, D.F. Strong and J.G. Thurlow. Geological Association of Canada, Special Paper 22, pages 205-228.

Horikoshi, E.
1969: Volcanic activity related to the formation of the Kuroko-type deposits in the Kosaka District, Japan. Mineralium Deposita, Volume 4, pages 321-345.

Jambor, J.L.
1987: Geology and origin of the orebodies in the Lucky Strike area. *In* Buchans Geology, Newfoundland. *Edited by* R.V. Kirkham. Geological Survey of Canada, Paper 86-24, pages 75-106.

Kirkham, R.V. and Thurlow, J.G.
1987: Evaluation of a resurgent caldera and aspects of ore deposition and deformation at Buchans. *In* Buchans Geology, Newfoundland. *Edited by* R.V. Kirkham. Geological Survey of Canada, Paper 86-24, pages 177-194.

McPhie, J., Doyle, M. and Allen, R.L.
1993: Volcanic textures: a guide to the interpretation of textures in volcanic rocks. Centre for Ore Deposit and Exploration Studies, University of Tasmania, Hobart, Australia, 198 pages.

Moore, P. and Butler, D.
2019: Assessment report on compilation, resource estimation, and geophysical and diamond drilling exploration for 2019 submission for fee simple grants volume 1 folios 61-62, and for first, second, fifth, sixth, twelfth, thirteenth and fourteenth year assessment for licences 10524M, 10525M, 11431M, 11432M, 11796M, 13320M, 13423M, 13539M, 20606M, 21328M, 22209M, 22211M, 22213M, 22224M, 22682M, 25434M and 26626M on claims in the Red Indian Lake Area, Buchans, central Newfoundland. Newfoundland and Labrador Geological Survey, Assessment File 12A/1880, 1547 pages.

Moore, P., Butler, D., Webster, P.C., Barr, P.J.F., Hearst, R., Lambert, G. and O'Brien, P.J.
2009: Assessment report on compilation, resource estimation, and geophysical and diamond drilling exploration for 2008 submission for fee simple grants volume 1 folios 61-62, and for second, third, fourth, thirteenth and sixteenth year assessment for licences 5668M, 8295M, 10452M-10453M, 10524M-10526M, 10546M-10548M, 10551M, 11431M-11433M, 11793M-11799M, 11801M, 11808M, 13320M, 13423M and 13539M on claims in the Buchans Area, central Newfoundland, 5 reports. Newfoundland and Labrador Geological Survey, Assessment File 12A/15/1368, 1377 pages.

Pontual, S., Merry, N. and Gamson, P.
1997: G-Mex volume 1: Spectral interpretation field manual; Arrowtown, New Zealand, AusSpec International Pty. Ltd., 86 pages.

Saunders, P., Harris, J., Wilton, D.H.C. and Winter, L.S.
2000: Assessment report on geochemical exploration for 2000 submission for fee simple grants volume 1 folios 61-62 and for first year and first year supplementary to seventh year supplementary assessment for licence 4273 on claim block 7915, licence 4293 on claim block 7898, licence 4294 on claim block 7896, licence 4317 on claim block 7984, licence 4319 on claim blocks 6663-6664 and 7793-7794, licence 4547 on claim 16171, licence 4548 on claim 16507, licence 4603 on claim 16946, licence 4744 on claim 16406-16407, licence 4793 on claims 16420-16421, licence 4805 on claim 16398, licence 4806 on claims 16397, 16399-16401, 16424-16426 and 17686-17688, licence 4823 on claims 16431-16432, licence 4858 on claim blocks 7919-7921 and claims 16512 and 16514, licence 4859 on claim blocks 7916-7917 and claims 16513 and licences 4973M, 5649M, 5668M, 6003M, 6712M, 7319M and 7420M on claims in the Buchans area, central Newfoundland, 2 reports. Newfoundland and Labrador Geological Survey, Assessment File 12A/15/0951, 197 pages.

Saunders, P., Harris, J., Winter, L., Wilton, D.H.C., Spurvey, P. and Scott, W. J.
1998: First, third, fourth and fifth year assessment report on geochemical, geophysical and diamond drilling exploration for licence 4273 on claim block 7915, licence 4293 on claim block 7898, licence 4294 on claim block 7896, licence 4295 on claim block 7855, licence 4470 on claim block 4919, licence 4497 on claim 16090, licence 4547 on claim 16171, licence 4603 on claim 16496, licence 4744 on claim 16406, licence 4805 on claim 16398 and licences 5574m, 5649m-5651m and 6003m on claims in the Buchans area, central New-foundland, 6 reports. Newfoundland and Labrador Geological Survey, Assessment File 12A/15/0854, 399 pages.

Saunders, P., Scott, W.J. and Laletsang, K.B.
1996: First, second and third year assessment report on geological, geochemical, geophysical and diamond drilling exploration for licence 4294 on claim block 7896, licence 4295 on claim block 7855, licence 4470 on claim block 4919, licence 4547 on claim 16171, licence 4603 on claim 16496 and licence 4744 on claims 16406-16407 in the Buchans Brook, Middle Branch, East Branch and Woodmans Brook areas, central Newfoundland, 2 reports. Newfoundland and Labrador Geological Survey, Assessment File 12A/15/0753, 169 pages.

Sparkes, G.W.
2022: Short wavelength infrared spectrometry studies of sericitic alteration zones, southern Buchans–Roberts Arm Belt, Newfoundland. *In* Current Research. Government of Newfoundland and Labrador, Department of Industry, Energy and Technology, Geological Survey, Report 22-1, 34 pages.

Sparkes, G.W. and Hamilton, M.A.
This volume: New U–Pb age constraints on key units within the Buchans camp, southern Buchans–Roberts Arm Belt, central Newfoundland.

Sparkes, G.W., Hamilton, M.A. and Dunning, G.R.
2021: Age constraints on VMS mineralization, central Buchans–Roberts Arm Belt, Newfoundland. *In* Current Research. Government of Newfoundland and Labrador, Department of Industry, Energy and Technology, Geological Survey, Report 21-1, 16 pages.

Sparkes, G.W. and Hinchey, J.G.
2023: White mica zonation patterns associated with hybrid bimodal-felsic VMS systems: Examples from the Tulks Volcanic and Buchans–Roberts Arm belts, central Newfoundland. *In* Current Research. Government of Newfoundland and Labrador, Department of Industry, Energy and Technology, Geological Survey, Report 23-1, 27 pages.

Swinden, H.S., Jenner, G.A. and Szybinski, Z.A.
1997: Magmatic and tectonic evolution of the Cambrian-Ordovician margin of Iapetus: geochemical and isotopic constraints from the Notre Dame Subzone, Newfoundland. *In* Nature of Magmatism in the Appalachian Orogen. *Edited by* A.K. Sinha, J.B. Whalen and J.P. Hogan. Geological Society of America, Memoir 191, pages 337-365.

Thurlow, J.G.
1981: Geology, Ore Deposits and Applied Rock Geochemistry of the Buchans Group, Newfoundland. Unpublished Ph.D. Thesis, Memorial University of Newfoundland, St. John's, Newfoundland.

2001: Geology of the Buchans Orebodies – A 1999 Summary. *In* GAC Field Trip Guide Book, Field Trip A2 (Part 1) Geology and Mineral Deposits of the Northern Dunnage Zone, Newfoundland Appalachians. *Edited by* D.T.W. Evans and A. Kerr. Geological Association of Canada, Field Trip Guidbook, pages 155-163.

Thurlow, J.G. and Swanson, E.A.
1981: Geology and ore deposits of the Buchans area, central Newfoundland. *In* The Buchans Orebodies: Fifty Years of Mining and Exploration. *Edited by* E.A. Swanson, D.F. Strong and J.G. Thurlow. Geological Association of Canada, Special Paper 22, pages 113-142.

1987. Stratigraphy and structure of the Buchans Group. *In* Buchans Geology, Newfoundland. *Edited by* R.V. Kirkham. Geological Survey of Canada, Paper 86-24, pages. 35-46.

Thurlow, J.G., Spencer, C.P., Boerner, D.E., Reed, L.E. and Wright, J.A.
1992: Geological interpretation of a high resolution reflection seismic survey at the Buchans mine, Newfoundland. Canadian Journal of Earth Sciences, Volume 29, pages 2022-2037.

van Hees, G.W.
2011: Chemostratigraphy and Alteration Geochemistry of the Lundberg and Engine House Volcanogenic Massive Sulfide Mineralization, Buchans, Central Newfoundland. Unpublished M.Sc. Thesis, University of Ottawa, Ottawa, Ontario.

Whalen, J., Zagorevski, A., McNicoll, V.J. and Rogers, N.
2013: Geochemistry, U–Pb geochronology, and genesis of granitoid clasts in transported volcanogenic massive sulfide ore deposits, Buchans, Newfoundland. Canadian Journal of Earth Sciences, Volume 50, pages 1116-1133.

Winter, L.S.
2000: Derivation of Base-line Geochemistry, Petrography, and Isotopic Data from the Host Rocks to the Lucky Strike Deposit and Comparison with Data from other Alteration Zones, Buchans Mining Camp, Newfoundland. Unpublished M.Sc. Thesis, Memorial University of Newfoundland, St. John's, NL.

Zagorevski, A. and Rogers, N.
2008: Stratigraphy and structural geology of the Ordovician volcano-sedimentary rocks in the Mary March Brook area. *In* Current Research. Government of Newfoundland and Labrador, Department of Natural Resources, Geological Survey, Report 8-1, pages 101-113.

2009: Geochemical characteristics of the Ordovician volcano-sedimentary rocks in the Mary March Brook area. *In* Current Research. Government of Newfoundland and Labrador, Department of Natural Resources, Geological Survey, Report 9-1, pages 271-288.

Zagorevski, A., McNicoll, V., van Staal, C.R., Kerr, A. and Joyce, N.
2015: From large zones to small terranes to detailed reconstruction of an Early to Middle Ordovician arc-backarc system preserved along the Iapetus suture zone: a legacy of Hank Williams. Geoscience Canada, Volume 42, pages 125-150.

Zagorevski, A., McNicoll, V.J., Rogers, N. and van Hees, G.H.
2016: Middle Ordovician disorganized arc rifting in the peri-Laurentian Newfoundland Appalachians: Implications for evolution of intra-oceanic arc systems. Journal of the Geological Society, Volume 173, pages 76-93.

Zagorevski, A., Rogers, N., van Staal, C., McClenaghan, S. and Haslam, R.
2007: Tectonostratigraphic relationships in the Buchans area: A composite of Ordovician and Silurian terranes? Government of Newfoundland and Labrador, Department of Natural Resources, Geological Survey, Report 7-1, pages 103-116.